Clemson University
TigerPrints

All Theses | Theses

12-2008

# INDEPENDENT TORQUE DISTRIBUTION MANAGEMENT SYSTEMS FOR VEHICLE STABILITY CONTROL

Indrasen Karogal
*Clemson University*, ikarogal@yahoo.com

Follow this and additional works at: https://tigerprints.clemson.edu/all_theses

 Part of the Engineering Mechanics Commons

Recommended Citation
Karogal, Indrasen, "INDEPENDENT TORQUE DISTRIBUTION MANAGEMENT SYSTEMS FOR VEHICLE STABILITY CONTROL" (2008). *All Theses*. 490.
https://tigerprints.clemson.edu/all_theses/490

This Thesis is brought to you for free and open access by the Theses at TigerPrints. It has been accepted for inclusion in All Theses by an authorized administrator of TigerPrints. For more information, please contact kokeefe@clemson.edu.

# INDEPENDENT TORQUE DISTRIBUTION MANAGEMENT SYSTEMS FOR VEHICLE STABILITY CONTROL

---

A Thesis
Presented to
the Graduate School of
Clemson University

---

In Partial Fulfillment
of the Requirements for the Degree
Master of Science
Mechanical Engineering

---

by
Indrasen Suresh Karogal
December 2008

---

Accepted by:
Dr. Beshah Ayalew, Committee Chair
Dr. Harry Law
Dr. Pierluigi Pisu

# ABSTRACT

Vehicle Dynamics Control (VDC) systems, also called Electronic Stability Control (ESC) systems, are active on-board safety systems intended to stabilize the dynamics of vehicle lateral motion. In so doing, these systems reduce the possibility of the driver's loss of control of the vehicle in some critical or aggressive maneuvers. One approach to vehicle dynamics control is the use of appropriate drive torque distribution to the wheels of the vehicle. This thesis focuses on particular torque distribution management systems suitable for vehicles with independently driven wheels.

In conducting this study, a non-linear seven degree-of-freedom vehicle model incorporating a non-linear tire model was adopted and simulated in the MATLAB/SIMULINK environment. Using this model, various VDC torque management architectures as well as choices of feedback controllers were studied. For the purposes of upper level yaw stability control design, the desired or reference performance of the vehicle was obtained from the steady state bicycle model of the vehicle.

To achieve the corrective yaw moment required for directional control, four torque distribution strategies were devised and evaluated. For each strategy, the following feedback control variables were considered turn by turn: 1) yaw rate 2) lateral acceleration 3) both yaw rate and lateral acceleration. Standard test maneuvers such as fish hook maneuver, the FMVSS 126 ESC test and the J-turn were simulated to evaluate the effectiveness of the proposed torque distribution strategies. Effects of road friction conditions, yaw-controller gains, and a driver emulation speed controller were also

studied. The simulation results indicated that all VDC torque management strategies were generally very effective in tracking the reference yaw rate and lateral acceleration of the vehicle on both dry and slippery surface conditions. Under the VDC strategies employed, the sideslip angle of the vehicle remained very small and always below the steady-state values computed from reference bicycle model. This rendered separate side slip angle control unnecessary, for the test conditions and test vehicle considered.

The study of the various proposed independent torque control strategies presented in this thesis is an essential first step in the design and selection of actuators for vehicle dynamics control with independent wheel drives. This is true for certain power train architectures currently being considered for pure Electric or Hybrid Electric and Hydraulic Hybrid Vehicles.

# DEDICATION

This thesis is dedicated to my parents, Mr. Suresh Vithalrao Karogal and Mrs. Anagha Karogal, who gave me the opportunity to come to the United States for advanced education and my elder sister, Mrs. Anuja Deshpande without whose unconditional love and support this thesis would not be complete.

# ACKNOWLEDGMENTS

I would like to express my sincere gratitude to my research advisor, Dr. Beshah Ayalew for his invaluable guidance, continuous inspiration and encouragement for the completion of this thesis and financial support throughout my graduate study. I am grateful to Dr. Harry Law for his valuable advice and vital suggestions in carrying out this research. I am also thankful to Dr. Pierluigi Pisu for being a part of my committee and for his support and valuable suggestions.

I give my deep appreciation to all my office-mates, friends and my room-mates who have inspired me in the research. A special thanks to Mr. Judhajit Roy for his help during the course of this work. I warmly thank my friends Mr. Aditya Bhandari, Mr. Tejas Ghotikar, Ms. Gauri Phadke, Mr. Souharda Raghavendra, Mr.Saurabh Keni, Ms. Niraja Gokhale, Mr. Kushan Vora, Mr. Ankur Sonawane and fellow graduate student Mr. Santosh Tiwari for their advice and friendly help.

## TABLE OF CONTENTS

Page

TITLE PAGE……i

ABSTRACT.....…...i

DEDICATION……iv

ACKNOWLEDGEMENTS……v

TABLE OF CONTENTS……....vi

LIST OF TABLES……..ix

LIST OF FIGURES……x

CHAPTER……...1

I. INTRODUCTION…….....1

Vehicle Stability Control.…….....1
Thesis Outline ……5

II. DYNAMIC SYSTEM MODELING……..7

Vehicle Model……..7
Vehicle Dynamics Control……14
Chapter Summary……..20

III. VEHICLE DYNAMICS CONTROL VIA TORQUE DISTRIBUTION MANAGEMENT…….……21

Yaw Moment Control through Torque Transfer……21
Torque Distribution Approaches……22
Chapter Summary……..32

IV. RESULTS AND DISCUSSIONS…….33

Selection of Test Maneuver……...33
Simulation of Road Surface Conditions……37
Yaw Rate Control…….....37
VDC for Sudden Changes in Steering Input (J-turn)…….....44

Table of Contents (Continued)

Lateral Acceleration Control...……..55
Combined Control (Feedback Control Using Yaw Rate
and Lateral Acceleration both)...…….....57
Comparisons (Yaw Rate Control Vs. Lateral Acceleration
Control Vs. Combined Control)…….59
Need of Slip Control…….……63
Chapter Summary…..……....64

V. CONCLUSIONS AND FUTURE WORK……...66

Summary and Conclusions……66
Future Work……...……...68

APPENDIX…….....70

PACEJKA TIRE MODEL: LATERAL FORCE,
AND LONGITUDINAL FORCE…….70

REFERENCES…….....73

NOMENCLATURE……..75

SUBSCRIPTS……77

# LIST OF TABLES


| Table | | Page |
|---|---|---|
| 1 | Vehicle Performance for Different Controller Strengths: Yaw Rate feedback……...…….....42 | |
| 2 | Comparison of VDC Strategies: Yaw Rate Error Feedback.....49 | |

# LIST OF FIGURES


| Figure | | Page |
|---|---|---|
| 1 | Basic Functioning of ESC……....3 | |
| 2 | Schematic of Vehicle Model: Longitudinal and Lateral dynamics……..8 | |
| 3 | Forces at the road wheel interface a) Forces in the wheel fixed co-ordinate system b) Forces in the body fixed co-ordinate system.……...9 | |
| 4 | Free Body Diagram of Sprung Mass of Vehicle……....11 | |
| 5 | Rotational Dynamics of Wheel……..……12 | |
| 6 | Kinematics of Wheels and Co-ordinate Transformations…..……13 | |
| 7 | Schematic of Non-linear Vehicle Model in MATLAB SIMULINK Environment……..15 | |
| 8 | Flow Diagram of Generalized Structure of VDC…..……16 | |
| 9 | Schematic of ESC Control Architecture……20 | |
| 10 | Torque Ratio Approach for VDC……..25 | |
| 11 | Schematic of Vehicle in Various Scenarios and Adopted Sign Conventions in Steady state……27 | |
| 12 | Modified NHTSA Fish hook Maneuver Test Input……...35 | |
| 13 | FMVSS 126 VDC Test Steer Input…….....37 | |
| 14 | Step Steer Input for RWA = 3 deg…….38 | |

15 Yaw Rate Time History Plot (VDC Controlled System Vs. Desired) Torque Distribution Strategy 4 with Speed Control: Dry surface (μ = 1)……...39

16 Lateral Acceleration Vs. Time (VDC Controlled System Vs.Desired) Torque Distribution Strategy 4 with Speed Control: Dry surface (μ = 1)……...39

17 Vehicle Sideslip Angle Vs. Time (VDC Controlled System Vs. Desired)……...40

18 Individual Final Wheel Torques of VDC Controlled Vehicle Torque Distribution Strategy 4 with Speed Control: Dry surface ($\mu = 1$) ……..41

19 Individual Wheel Slips (VDC: Yaw Control)……42

20 Yaw Rate Response (VDC Controlled and Uncontrolled) Torque Distribution Strategy 4: Dry surface ($\mu = 1$)……43

21 Lateral Acceleration Response (VDC Controlled and Uncontrolled) Torque Distribution Strategy 4 with Speed Control: Dry surface ($\mu = 1$)……44

22 Yaw Rate Response to Step Steer of 3 deg RWA (VDC Controlled and Uncontrolled) Torque DistributionStrategy 4 with Speed Control: Dry surface ($\mu = 1$)……...43

23 Lateral Acceleration Response to Step Steer of 3 deg RWA (VDC Controlled and Uncontrolled) Torque Distribution Strategy 4 with Speed Control: Dry surface ($\mu = 1$)……45

24 Sideslip angle Response to Step Steer of 3 deg RWA (VDC Controlled and Uncontrolled) Torque Distribution Strategy 4 with Speed Control: Dry Surface ($\mu = 1$)……...45

25 Yaw Rate Response: Comparison of Controller Gains (Yaw Rate Error Feedback: Dry surface ($\mu = 1$))……..47

26 Torques on Front left Wheel: Comparison of Controller Gains (Yaw Rate Error Feedback: Dry surface ($\mu = 1$))……..48

27 Yaw Rate Response: Comparison of VDC Strategies……...49

28 Lateral Acceleration Response: Comparison of VDC Strategies (Yaw Rate Error Feedback with Speed Control: Dry surface($\mu = 1$)))…….50

29 Torques on Front left Wheel: Comparison of VDC Strategies (Yaw Rate Error Feedback with Speed Control: Dry surface($\mu = 1$)))…….....50

30 Final Torques on individual wheels: Comparison of VDC Strategies (Yaw Rate Error Feedback with Speed Control: Dry surface ($\mu = 1$)))…….51

31 Sideslip Angle Response: Comparison of VDC Strategies (Yaw Rate Error Feedback with Speed Control: Dry surface ($\mu = 1$)))……53

32 Yaw Rate Response: Comparison of VDC Strategies (Yaw Rate Error Feedback with No speed control: Dry surface ($\mu = 1$)))…….....55

33 Resultant Torques on Individual Wheels: Comparison of VDC Strategies (Yaw Rate Error Feedback with No speed control: Dry surface ($\mu = 1$)))…….56

34 Yaw Rate Response (Lateral Acc. Error Feedback with Speed Control on Slippery surface (μ = 0.3))……57

35 Lateral Acceleration Response (Lateral Acc. Error Feedback with Speed Control on Slippery surface (μ = 0.3))……57

36 Sideslip Angle Response (Lateral Acc. Error Feedback with Speed Control on Slippery surface ($\mu = 0.3$))……57

37 Resultant Torques on Individual Wheels (Lateral Acc. Error Feedback with Speed Control on Slippery surface ($\mu = 0.3$))……58

38 Yaw Rate Response (Combined (Yaw Rate and Lateral Acc.) Error Feedback with Speed Control on Slippery surface ($\mu = 0.3$))……59

39 Lateral Acceleration Response (Combined (Yaw Rate and Lat. Acc.) Error Feedback with Speed Control on Slippery surface ($\mu = 0.3$))……59

40 Sideslip Angle Response (Combined (Yaw Rate and Lat. Acc.)Error Feedback with Speed Control on Slippery surface ($\mu = 0.3$))……59

41 Resultant Torques on Individual Wheels (Lateral Acc. Error Feedback with Speed Control on Slippery surface ($\mu = 0.3$))……60

42 Yaw Rate Response: Comparison of Feedback Control Techniques (Slippery surface ($\mu = 0.3$) without speed control)……61

43 Lateral Acceleration Response: Comparison of Feedback Control Techniques (Slippery surface ($\mu = 0.3$) without speed control)……62

44 Sideslip Angle Response: Comparison of Feedback Control Techniques……63

45 Torques on individual wheels: Comparison of Feedback Control Techniques (Slippery surface ($\mu = 0.3$) without speed control)……64

46 Longitudinal Force Coeff. Vs Longitudinal Slip Ratio: Dry surface ($\mu = 1$)……65

# CHAPTER 1

# INTRODUCTION

## 1.1 Vehicle Stability Control

Vehicle safety systems have evolved significantly in the past two decades. These safety systems are classified into passive systems (those that protect occupants in the event of an accident) and active systems (those that prevent the accidents by active intervention as pre-crash measures). One of the main trends in the recent development of vehicle safety systems is Vehicle Dynamics Control (VDC) to maintain vehicle stability.

VDC, also called Electronic Stability Control (ESC), is an active safety system designed to reduce loss of control by correcting the onset of vehicle instability. It has the potential to provide benefits in many driving scenarios and road surface conditions where average drivers may not be able to recognize and react appropriately to correct severe understeering and oversteering of the vehicle. A number of studies suggest that VDC has the potential to reduce crashes resulting from such loss of control (1), (2), (3). ESC reduces the occurrence of crashes with personal injuries, especially fatal and serious injuries. If all vehicles were to be fitted with VDC systems, nearly one-third of all fatal crashes could be prevented and rollover risk can be reduced by as much as 80% as reported by the Insurance Institute for Highway Safety (3) .

The need for VDC arises from situations involving non-linear changes in tire slip angles. The tire slip angles, and consequently, the vehicle slip angle might increase rapidly without a corresponding increase or even decrease in lateral forces if a vehicle

reaches its physical limit of adhesion between the tires and the road (4). The sensitivity of yaw moment to changes in steering angle becomes highly reduced. In other words, the effect of a given steering angle depends on the actual side slip angle (5), (6). On dry asphalt, vehicle maneuverability is typically lost at vehicle slip angles greater than ten degrees while on packed snow, vehicle maneuverability is lost at slip angles as low as four degrees (5). Average drivers have experience in operating the vehicle in its linear range in which a given steering wheel movement produces a proportional change in the vehicle's heading. But at the limits of adhesion between the tires and road, they don't recognize the change in the friction coefficient and have no information of the vehicle's stability margin (6). During such situations, most drivers may start to panic and may react in a wrong way by steering too much.

The goal of vehicle stability enhancement systems is to bring the vehicle into predictable regime of vehicle behavior so that drivers could maintain better control of the vehicle.

The control strategy behind current vehicle stability control systems is to generate required corrective yaw moment in various ways and thus to reduce the deviation of vehicle behavior from its normal behavior. A typical example of the basic working of ESC systems is depicted in Figure (1).

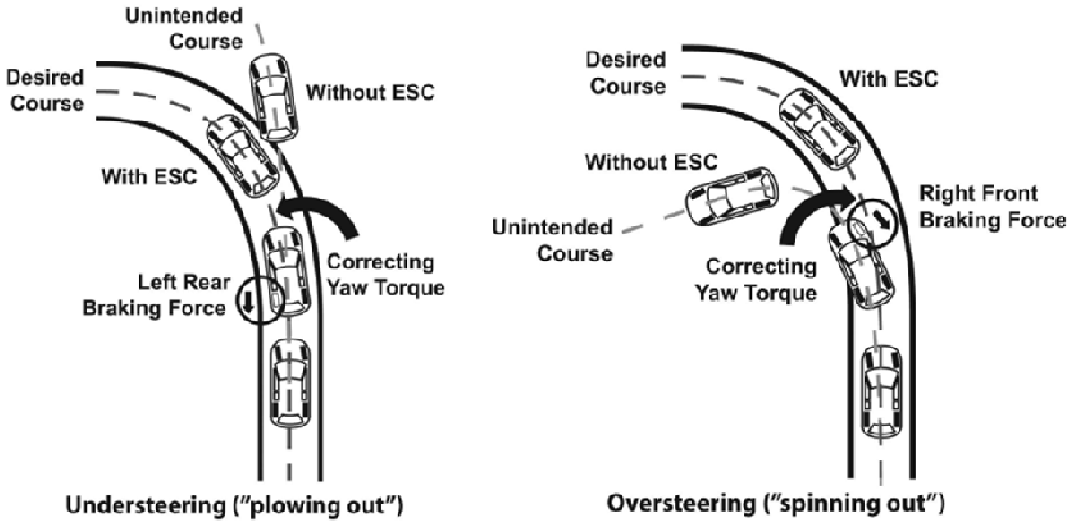


Figure 1 Basic Functioning of ESC, (20)

as (7):

1. Differential Braking Systems: In these systems, the required yaw moment is generated by applying differential braking between left and right wheels.

2. Steer-by-Wire Systems: These systems modify the driver's steering angle input and add a correction steering angle..

3. Active Torque-Distribution Systems: These systems can be: (a) torque vectoring systems which utilize the active differentials for varying the torque split through powertrain to achieve the desired yaw moment control or, (b) independent traction control systems which adopt all wheel drive technology to independently control the drive torque distributed to each wheel. A higher degree of freedom in the distribution of

torques has been achieved by torque biasing differentials (8) and use of twin couplings which independently control the torque to each wheel of an axle (9).

Most vehicle stability control systems in the market today are brake-based. With these brake-based strategies the vehicle speed is compromised. By comparison, the torque distribution based yaw moment control has a better vehicle speed performance and is gaining more visibility.

Further enhancement in the flexibility in the distribution of torque can be made possible by fully independent drive torque distribution. It was noted that the emphasis of Four-Wheel Drive (4WD) or All-Wheel Drive (AWD) systems has shifted from traction performance enhancement to on-road stability and handling performance improvement (10). Advancement in all-wheel drive technology has made the idea of independent control of drive torque to each wheel realizable.

The motive behind this thesis is to research the design of a Vehicle Dynamics Control system that enables independent torque control of each wheel of the vehicle using independent in-wheel motors. Emphasis on energy-saving and reduction in environmental pollution have been forcing the automotive industry to reduce exhaust emissions and achieve better fuel economy. The has led to the accelerated research and development of hybrid electric vehicles (HEVs), electric vehicles (EVs) fuel cell vehicles (FCVs), and hydraulic hybrid vehicles (HHVs) a) Electric or hydraulic propulsion systems employed in these vehicles can be configured with independent in-wheel or on-board drive motors (11), (12).

That is, the electric or hydraulic motors of the powertrain in these vehicles can be integrated into each wheel or can drive each wheel independently and can be controlled independently (13), (14). These drive configurations allow the possibility of vehicle dynamics control by proportioning vehicle tractive forces via the torque applied at each drive wheel. The high controllability of electric or hydraulic motors (via the manipulation of their torque outputs) offers an opportunity to employ vehicle dynamics control by modulating the independent drive torque for such EVs, HEVs, FCVs or HHVs. This research is primarily concerned with the study of vehicle dynamics control architectures for such vehicles. The various architectures will be referred to as independent torque distribution management systems for vehicle stability. The study proposes and evaluates various proposed independent torque distribution strategies and would help in design and selection of in-wheel hydraulic or electric motors for use in EVs, HEVs, FCVs or HHVs.

## 1.2 Thesis Outline:

The following paragraphs describe the outline of this thesis. The organization of chapters and the contributions of each chapter are explained in brief:

In Chapter 2, mathematical modeling of the vehicle used for the development and analysis of the proposed stability control strategies is presented. The chapter details the non-linear vehicle model and the Pacejka tire model adopted. It also includes a discussion of the vehicle dynamics control (VDC) strategies developed..

In Chapter 3, the design of the controller for VDC is described in detail. The physics behind yaw moment control through transfer of longitudinal forces is described followed

by discussion of an existing torque ratio approach for distribution of torque. The chapter focuses on elaborating the *differential torque transfer* approach and the different torque distribution strategies possible within this approach.

Chapter 4 discusses computer simulation results obtained from implementing the different torque distribution strategies discussed in Chapter 3. The chapter begins with the selection of test maneuvers for simulations. This is followed by the simulation results for steering inputs obtained corresponding to a modified fish-hook maneuver. The simulation results for different torque distribution strategies and parameters like controller gains and controller efforts are compared.

Chapter 5 concludes the thesis and suggests directions for future research to further improve certain performance characteristics of independent torque distribution systems.

# CHAPTER 2

# DYNAMIC SYSTEM MODELING

In this chapter, a 7 DOF nonlinear lumped parameter vehicle model that is adopted and simulated in the MATLAB/SIMULINK environment is described... The model is used for the analysis of the independent traction control systems.

## 2.1 Vehicle Model

The vehicle model adopted includes longitudinal, lateral and yaw motions as well as the rotational dynamics of the four wheels. It ignores the presence of the suspension and so excludes the following dynamics: heave, pitch and roll of the vehicle. Figure 2 shows the free body diagram for the vehicle model adopted. $\delta_f$ is the steering angle for the front wheels, which is considered to be identical for each of the left and right wheels during high speed cornering.

The longitudinal and lateral equations of motion for a rigid vehicle in planar motion can be obtained by equating total forces acting on the body in the particular direction (longitudinal or lateral) with the total inertia force in the respective direction. The effective longitudinal acceleration $(a_x)$ includes components due to change in longitudinal velocity and effect produced due to the product of yaw rate and lateral velocity. Similarly the effective lateral acceleration $(a_y)$ can be obtained. The total yaw moment acting on the vehicle can be obtained by equating the product of yaw inertia $(I_{zz})$ and the yaw acceleration $(\ddot{\Psi})$ with the effective moment produced due to lateral and longitudinal forces and the aligning moments. These equations are given by:

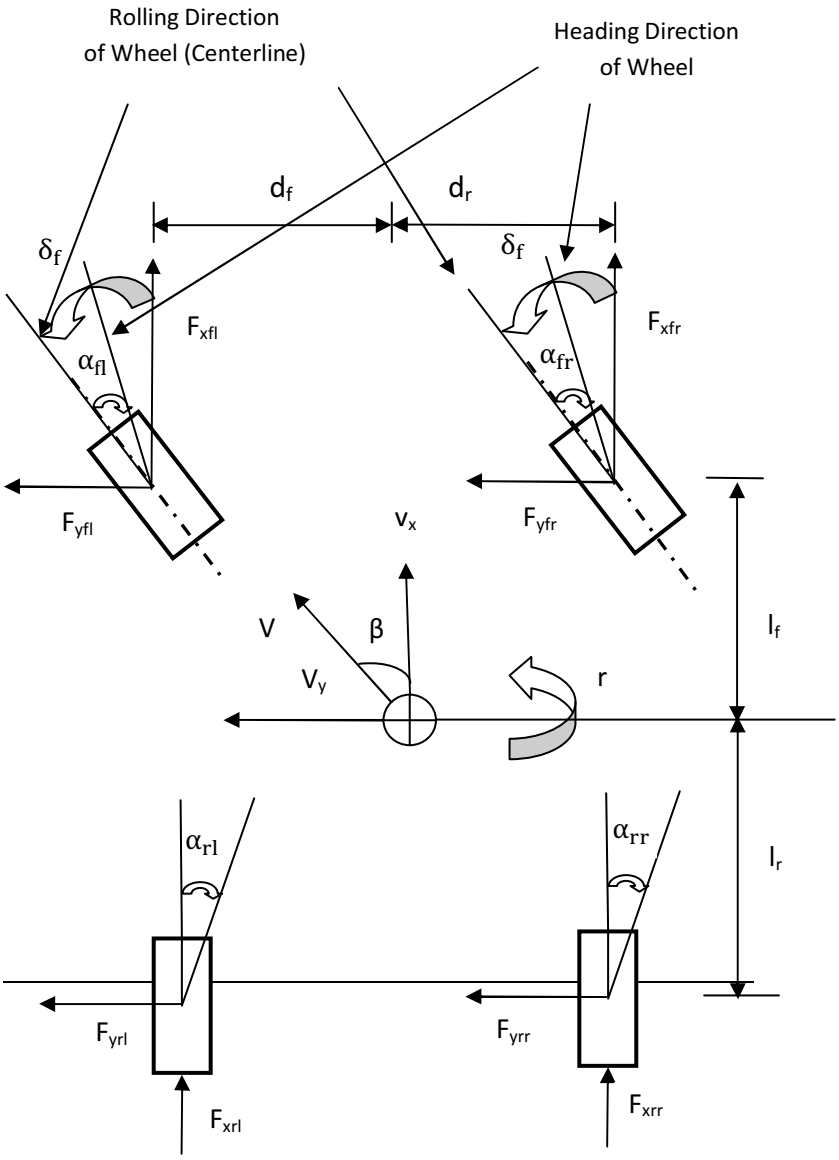


Figure 2 Free Body Diagram of Vehicle Model: Applied Forces (Plan View)

$$m\left(\underbrace{\dot{v}_x - \dot{\Psi} v_y}_{a_x}\right) = \sum F_x = F_{xfl_b} + F_{xfr_b} + F_{xrl_b} + F_{xrr_b} \tag{2.1}$$

$$m\underbrace{\left(\dot{v}_y + \dot{\Psi} v_x\right)}_{a_y} = \sum F_y = F_{yfl_b} + F_{yfr_b} + F_{yrl_b} + F_{yrr_b} \tag{2.2}$$

$$I_{zz}\ddot{\Psi} = \sum M_Z = l_f\left(F_{yfl_b} + F_{yfr_b}\right) - l_r\left(F_{yrl_b} + F_{yrr_b}\right) + \frac{d_f}{2}\left(F_{xfr_b} - F_{xfl_b}\right) +$$

$$\frac{d_r}{2}\left(F_{xrr_b} - F_{xrl_b}\right) + \sum_{i=1}^{4} M_{Zi} \qquad (2.3)$$

In the above equations, the lateral and longitudinal tire forces are given in terms of the body-fixed co-ordinate system and are represented with a suffix 'b' for body. However, the tire forces from Pacejka Model are given in a wheel-fixed co-ordinate system and are represented with a suffix 'w' for wheel. These forces in both these co-ordinate systems are shown in Figure 3.

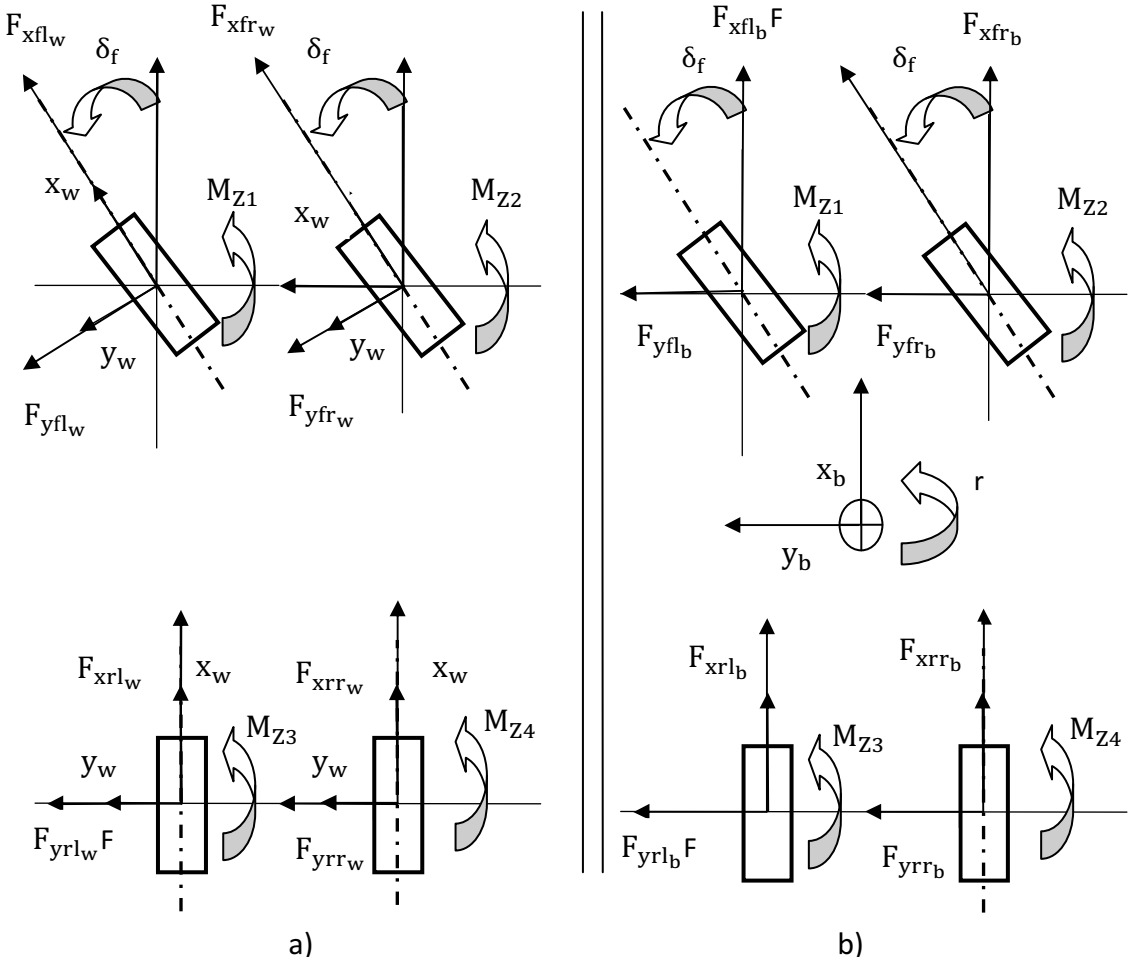


Figure 3 Forces at the Road Wheel Interface a) Forces in the Wheel Fixed Co-ordinate System b) Forces in the Body Fixed Co-ordinate System

The transformation of the forces between the two coordinate systems is given by:

$$F_{xfl_b} = F_{xfl_w}\cos\delta_f - F_{yfl_w}\sin\delta_f \quad (2.4)$$

$$F_{xfr_b} = F_{xfr_w}\cos\delta_f - F_{yfr_w}\sin\delta_f \quad (2.5)$$

$$F_{xrl_b} = F_{xrl_w} \quad (2.6)$$

$$F_{xrr_b} = F_{xrr_w} \quad (2.7)$$

$$F_{yfl_b} = F_{yfl_w}\cos\delta_f + F_{xfl_w}\sin\delta_f \quad (2.8)$$

$$F_{yfr_b} = F_{yfr_w}\cos\delta_f + F_{xfr_w}\sin\delta_f \quad (2.9)$$

$$F_{yrl_b} = F_{yrl_w} \quad (2.10)$$

$$F_{yrr_b} = F_{yrr_w} \quad (2.11)$$

## 2.2 Tire and Wheel Model

In this thesis, Pacejka (Magic Formula) formulations of tire models are used. The different forms are detailed in Appendix A, but the general form is:

$$Y(x) = D\sin\left(C\tan^{-1}\left\{Bx - E\left(Bx - \tan^{-1}(Bx)\right)\right\}\right) \quad (2.12)$$

where $Y(x)$ is either $F_x$ with x as longitudinal slip ratio S or $F_y$ with x as the lateral slip angle $\alpha$ or self-aligning moment $M_z$ with x the lateral slip angle $\alpha$. The coefficients in the above equation in each case depend on the tire design and road and load conditions.

There will certainly be normal forces acting on each wheel due to longitudinal and lateral accelerations ($a_x$ and $a_y$, respectively) of the vehicle. The corresponding normal reactions on the sprung mass of the vehicle are shown in the free body diagram of the sprung mass as shown in Figure 4.

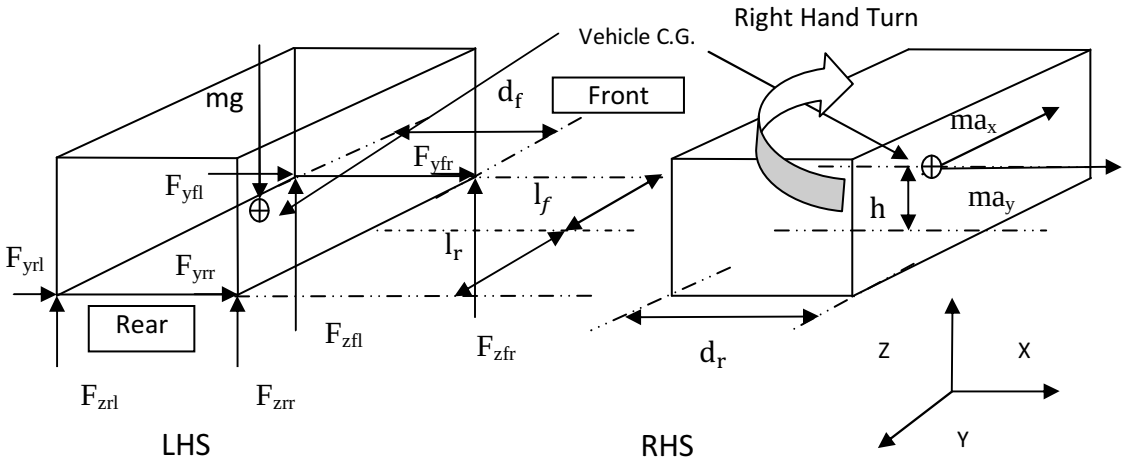


Figure 4 Free Body Diagram of Sprung Mass of vehicle

Neglecting suspension effects and solving the moment equations in X-Z plane, these normal forces are given by:

$$F_{zfl} = \frac{mgl_r}{2l} - \frac{ma_x h}{2l} - ma_y\left(\frac{l_r}{l}\right)\left(\frac{h}{d_f}\right) \tag{2.13}$$

$$F_{zfr} = \frac{mgl_r}{2l} - \frac{ma_x h}{2l} + ma_y\left(\frac{l_r}{l}\right)\left(\frac{h}{d_f}\right) \tag{2.14}$$

$$F_{zrl} = \frac{mgl_f}{2l} + \frac{ma_x h}{2l} - ma_y\left(\frac{l_f}{l}\right)\left(\frac{h}{d_r}\right) \tag{2.15}$$

$$F_{zrr} = \frac{mgl_f}{2l} + \frac{ma_x h}{2l} + ma_y\left(\frac{l_f}{l}\right)\left(\frac{h}{d_r}\right) \tag{2.16}$$

Each wheel in the vehicle model will have an angular acceleration corresponding to the torque on the wheel. These relevant equations are:

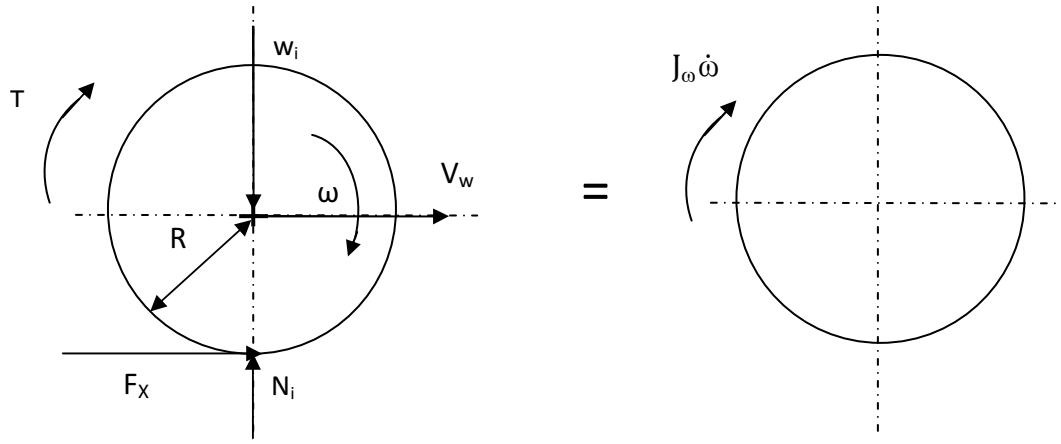


Figure 5 Rotational Dynamics of Wheel

$$T_{fl} - R_{fl} F_{xfl_w} = J_{\omega fl} \dot{\omega_{fl}} \quad (2.17)$$

$$T_{fr} - R_{fr} F_{xfr_w} = J_{\omega fr} \dot{\omega_{fr}} \quad (2.18)$$

$$T_{rl} - R_{rl} F_{xrl_w} = J_{\omega rl} \dot{\omega_{rl}} \quad (2.19)$$

$$T_{rr} - R_{rr} F_{xrr_w} = J_{\omega rr} \dot{\omega_{rr}} \quad (2.20)$$

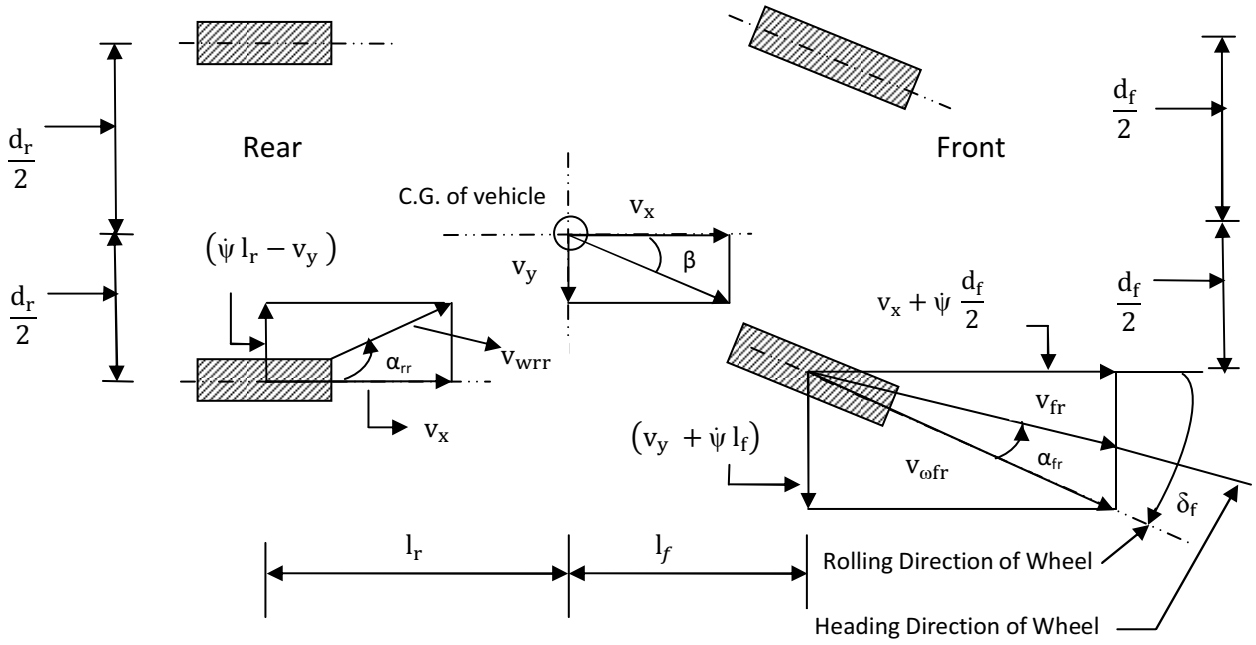


Figure 6 Kinematics of Wheels and Co-ordinate Transformations

The velocity of each wheel of the vehicle in the rolling direction of the wheel is given by (refer Figure 6):

$$v_{\omega fl} = \left(v_x - \dot{\psi}\,\frac{d_f}{2}\right)\cos\delta_f + \left(v_y + \dot{\psi}\,l_f\right)\sin\delta_f \tag{2.21}$$

$$v_{\omega fr} = \left(v_x + \dot{\psi}\,\frac{d_f}{2}\right)\cos\delta_f + \left(v_y + \dot{\psi}\,l_f\right)\sin\delta_f \tag{2.22}$$

$$v_{\omega lr} = \left(v_x + \dot{\psi}\,\frac{d_r}{2}\right) \tag{2.23}$$

$$v_{\omega rr} = \left(v_x - \dot{\psi}\,\frac{d_r}{2}\right) \tag{2.24}$$

The longitudinal slip ratio, S, at each ωheel is obtained from:

$$S_{\omega fl} = \left(\frac{R_{fl}\omega_{fl}}{v_{\omega fl}} - 1\right) \tag{2.25}$$

$$S_{\omega fr} = \left(\frac{R_{fr}\omega_{fr}}{v_{\omega fr}} - 1\right) \tag{2.26}$$

$$S_{\omega rl} = \left(\frac{R_{rl}\omega_{rl}}{v_{\omega rl}} - 1\right) \tag{2.27}$$

$$S_{\omega rr} = \left(\frac{R_{rr}\omega_{rr}}{v_{\omega rr}} - 1\right) \tag{2.28}$$

The slip angle, $\alpha$, for each wheel can be obtained from lateral and longitudinal components of the velocity at the wheel with respect to the C.G. of the vehicle.

$$\alpha_{fl} = \delta_f - \tan^{-1}\left(\frac{v_y + \dot{\psi}\, l_f}{v_x - \dot{\psi}\,\frac{d_f}{2}}\right) \tag{2.29}$$

$$\alpha_{fr} = \delta_f - \tan^{-1}\left(\frac{v_y + \dot{\psi}\, l_f}{v_x + \dot{\psi}\,\frac{d_f}{2}}\right) \tag{2.30}$$

$$\alpha_{rl} = -\tan^{-1}\left(\frac{v_y - \dot{\psi}\, l_f}{v_x - \dot{\psi}\,\frac{d_f}{2}}\right) \tag{2.31}$$

$$\alpha_{rr} = -\tan^{-1}\left(\frac{v_y - \dot{\psi}\, l_f}{v_x + \dot{\psi}\,\frac{d_f}{2}}\right) \tag{2.32}$$

The above set of equations (2.1- 2.32) describe a non-linear model of the vehicle system. These equations were implemented in the graphical programming interface of MATLAB/ SIMULINK. The schematic of the model is illustrated in Figure . It should be noted that, the equations can be suitably linearized to find eigenvalues and study the stability of the system.

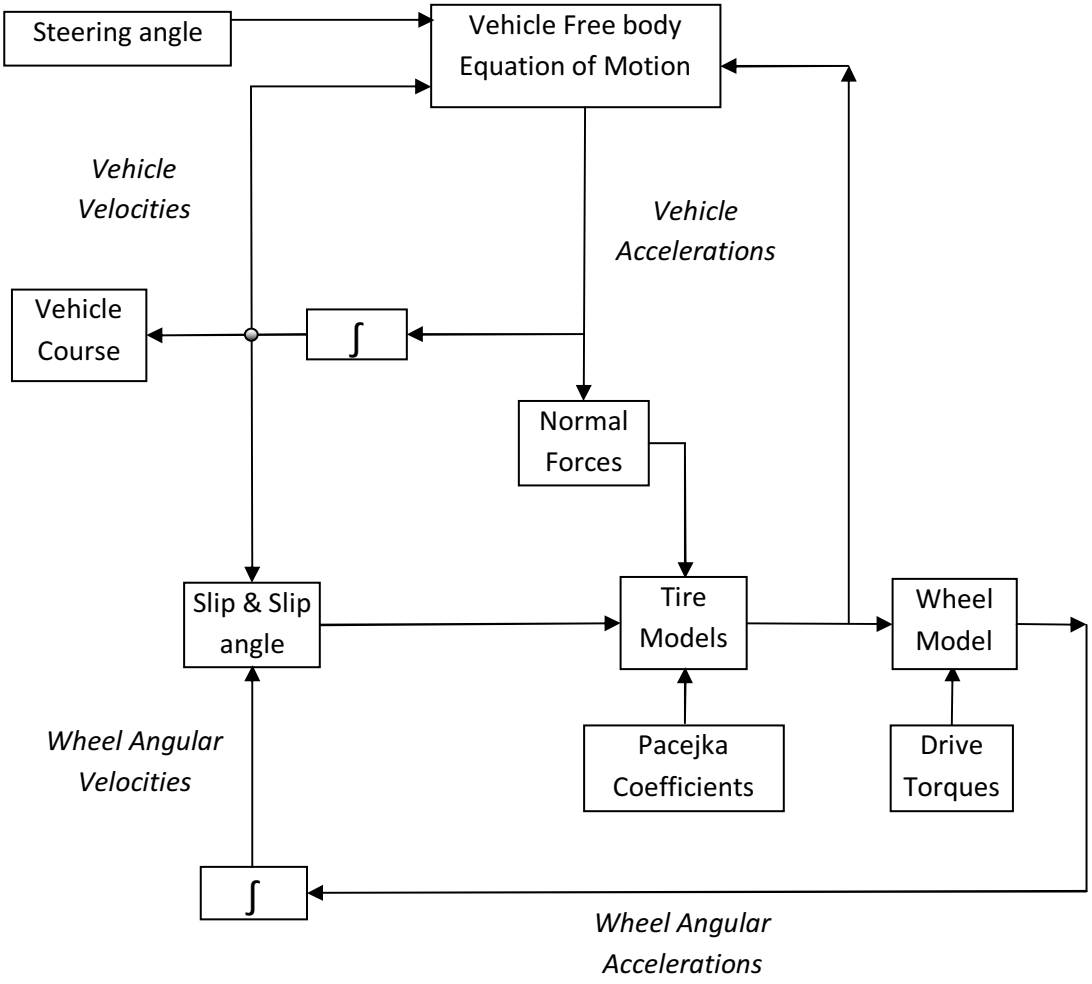


Figure **7** Schematic of Non-linear Vehicle Model in MATLAB/SIMULINK Environment, (18)

## 2.3 Vehicle Dynamics Control

The basic functionality of vehicle dynamics control (VDC) system involves reducing the deviation of the vehicle behavior from its normal behavior and maintaining the vehicle slip angle within specified bounds. A generalized structure of VDC system is shown in Figure .

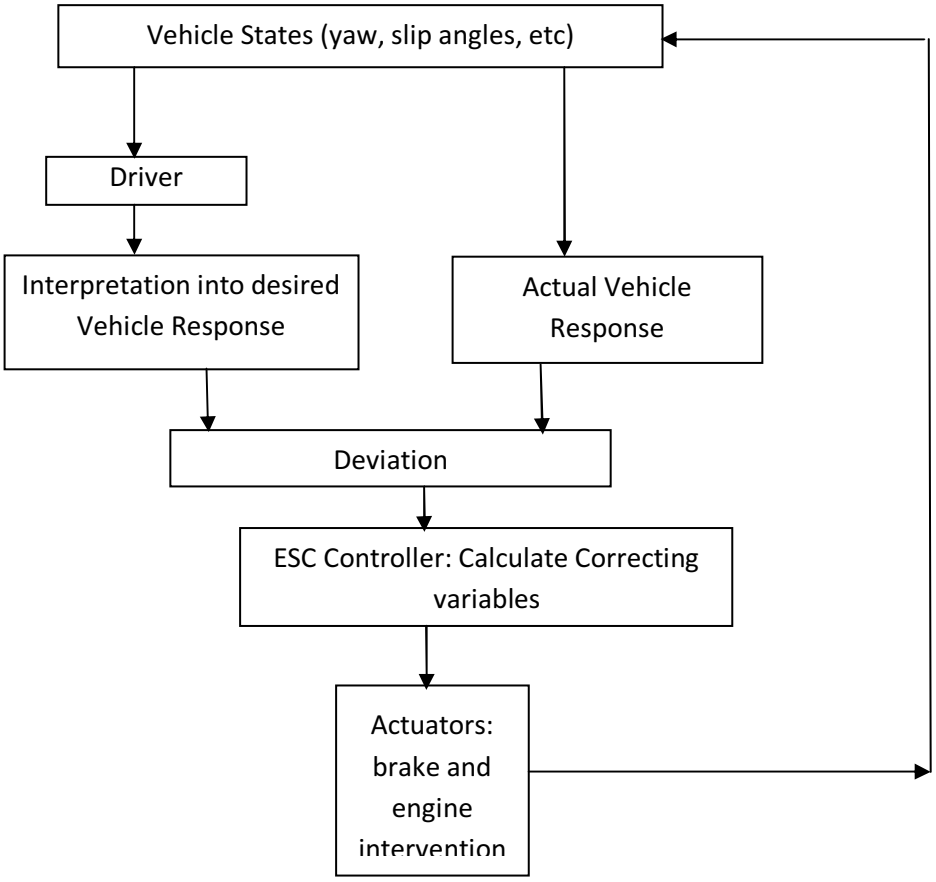


Figure 8 Flow Diagram of Generalized Structure of VDC

The vehicle dynamics controller (VDC) develops correcting variables like corrective yaw moment based on the deviation of desired and actual vehicle responses and passes this information to the actuators. The actuators (electric or hydraulic motors, braking systems etc.) manage the application and distribution of the required drive torque or braking effort to the wheels.

### 2.3.1 Actual Vehicle Responses

In practice, the actual vehicle responses can be obtained from the measurements and appropriate conversions from various mounted sensors like wheel speed sensors, yaw rate sensor, steering angle sensor, lateral accelerometers, and online estimators, if any. In the simulation study of this research, the non-linear vehicle model described in Section 2.1 is considered to give the actual vehicle responses.

### 2.3.2 Desired Responses for VDC

In practical VDC systems, the driver intended responses like steering input, torque and braking inputs can be use to estimate desired (target) vehicle responses based on a linearized and simplified model of the vehicle (15). In the simulation study of this research work, the desired responses are obtained from a bicycle model of the vehicle (which will be described later in this sub-section). The vehicle states considered in this study are the yaw rate, lateral acceleration and side slip angle of the vehicle. The VDC system is aimed at minimizing the need for the driver to act thoughtfully in panic situations. Considering this requirement, the driver has been deliberately excluded from all analysis of the VDC systems in this thesis.

The state space representation of the bicycle model used to generate desired or target responses is given by (16), (17):

$$\begin{bmatrix}\dot{\beta}\\ \dot{r}\end{bmatrix} = \begin{bmatrix}a11 & a12\\ a21 & a22\end{bmatrix}\begin{bmatrix}\beta\\ r\end{bmatrix} + \begin{bmatrix}b1\\ b1\end{bmatrix}\delta_f \tag{2.33}$$

where

$$a11 = -\left(\frac{C_1 + C_2}{m * v_x}\right)$$

$$a12 = -\left(1 + \frac{1}{m * {v_x}^2} * (C_1 * l_f - C_2 * l_r)\right)$$

$$a21 = -\left(\frac{l_f * C_1 - l_r * C_2}{I_{ZZ}}\right)$$

$$a22 = -\left(\frac{C_1 * {l_f}^2 + C_2 * {l_r}^2}{I_{ZZ} * v_x}\right)$$

$$b1 = \left(\frac{C_1}{m * v_x}\right)$$

$$b2 = \left(\frac{C_1 * l_f}{I_{ZZ}}\right)$$

In most cases, the desired responses of the state variables are chosen from steady state values of the bicycle model. For a given road wheel steering angle δ, the following desired states are defined (and can be extracted from the state space model given above):

1. Desired yaw rate ($r_d$) :

$$r_d = \frac{v_x * \delta}{1 + K_{us} * {v_x}^2} \tag{2.34}$$

2. Desired lateral acceleration $\left(a_{y_d}\right)$

$$a_{y_d} = \frac{{v_x}^2 * \delta}{1 + K_{us} * {v_x}^2} \tag{2.35}$$

3. Desired sideslip angle:

$$\beta_d = \left( \frac{l_f * l_r * \left( \frac{1}{l_f} - \frac{m * v_x^2}{l_r * C_2} \right) * \delta}{l^2 - m * \left( \frac{l_f}{C_2} - \frac{l_r}{C_1} \right) * v_x^2} \right) \quad (2.36)$$

The respective errors in some desired variables are defined as follows. The lateral acceleration error is:

$$e_{a_y} = a_y - a_{y_d} \quad (2.37)$$

The yaw rate error is:

$$e_r = r - r_d \quad (2.38)$$

$a_y$ and $r$ are the actual values of the corresponding vehicle states (lateral acceleration and yaw rate respectively) obtained from actual vehicle model. The lateral acceleration error, $e_{a_y}$ and yaw rate error $e_r$ are the feedback variables used in VDC design as will be detailed below.

### 2.3.3 Architecture of VDC

This sub-section describes the control architecture adopted in this research. This is depicted in Figure 9.

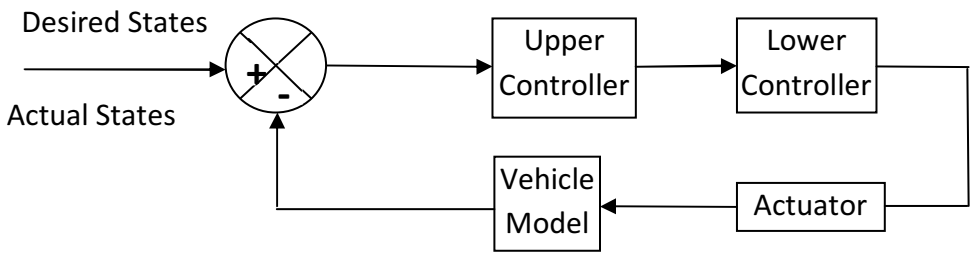


Figure 9 Schematic of ESC Control Architecture

#### 2.3.3.1 Upper Controller

The objectives of the upper controller are to ensure yaw stability control by commanding desired value of yaw moment and passing it to the lower controller. Inputs to the upper controller are the desired vehicle states defined in control law and the actual states of the vehicle. In this research, a PID controller is used as the upper controller to develop the corrective yaw moment which is then passed to the lower controller (explained in further detail in Chapter 3).

#### 2.3.3.2 Lower Controller

The lower (level) controller ensures that the corrective yaw moment demanded by the upper controller is converted to a demanded action on a lower level physical vehicle parameter. This parameter, which is generally a braking, driving or steering effort, should be properly controlled to achieve the desired corrective yaw moment with the appropriate actuation mechanism. In this research, the lower controller is the torque distribution management system that manages the torque distribution between the all wheels to

achieve the desired yaw moment. This lower level controller is explained in further detail in Chapter 3.

## 2.4 Chapter Summary

This chapter described the mathematical modeling of vehicle (7-DOF non-linear model). A generalized structure of VDC as studied in this research was described along with the discussion of how the desired states are extracted from the reduced bicycle model of the vehicle. The architecture of VDC as implemented in this research was also discussed. In the next chapter, the focus is on the lower level controller of the VDC architecture.

# CHAPTER 3

# Vehicle Dynamics Control via Drive Torque Distribution Management

In the previous chapter, the architecture of VDC and the concepts of upper and lower controllers were introduced. In this chapter, a corrective yaw-moment development system (upper controller design) and a torque distribution management system (lower controller design) are described in detail.

## 3.1 Yaw Moment Control through Torque Transfer

In this section, a physics- based description of the yaw moment control as achieved by differential torque management is described.

### 3.1.1 Front to Rear Torque Transfer

As more torque is transferred to the front, the longitudinal forces on the front wheels increase. In turn, the longitudinal slip of the front axle grows while that of the rear axle drops. This also leads to a decrease in the lateral forces generated by the front tires compared to the rear ones as explained by the friction ellipse (7), (16). Thus, increased torque transfer from the rear to the front wheels of the vehicle, induces an understeering effect.

### 3.1.2 Side to Side Torque Transfer:

The vehicle understeers when the driving torque on the outer wheel is reduced in comparison to that of the inner wheel due to generation of a yaw moment in the opposite direction of the turn. The longitudinal forces on the inner wheels increase while those on

the outer wheels decrease. Consequently, the lateral forces generated by inner wheels decrease while those of the outer wheels increase.

As explained by equation (2.3), the differences in longitudinal forces produce a significant yaw moment while the differences in lateral forces, being partially compensating, lead to generation of small positive yaw moments. Thus, a net positive yaw moment in the opposite direction of motion is generated, leading to understeer.

Active torque distribution systems utilize the physics described above for yaw moment control by varying the torques on individual wheels. In this research, yaw moment control through side to side torque transfer is proposed and various torque distribution approaches are considered and analyzed.

## 3. 2 Torque Distribution Approaches

Based on the physical consequence of longitudinal force distribution discussed in Section 3.1, two approaches of distribution of torque to each wheel of the vehicle are identified and explained in the following subsections.

### 3.2.1 Approach I: Variations in Torque Ratios

This approach as explained by Osborn and Shim (18), controls the two torque ratios using two feedback variables. The front- rear ratio of torques, $r_{fr}$ , is controlled by using one of the feedback variables, the yaw rate error, while the left-right ratio of torques, $r_{lr}$ , is controlled by lateral acceleration error. These torque ratios are defined as follows. The front-rear torque ratio is the ratio of the wheel torque on the front left wheel to the sum of wheel torques on front left and rear left wheels. It is also the ratio of wheel

torque on front right wheel to the sum of wheel torque on rear left and rear right wheels. Similarly, the left-right torque ratio is the ratio of wheel torque on the front left wheel to the sum of wheel torques on front left and front right wheels. It is also the ratio of wheel torque on front rear left wheel to the sum of wheel torque on rear left and rear right wheels These ratios are mathematically expressed in the equations given below.

$$r_{fr} = \frac{T_{fl}}{T_{fl}+T_{rl}} = \frac{T_{fr}}{T_{fr}+T_{rr}} \tag{3.1}$$

$$r_{lr} = \frac{T_{fl}}{T_{fl}+T_{fr}} = \frac{T_{rl}}{T_{rl}+T_{rr}} \tag{3.2}$$

Given a total driveline torque T, using the above definitions of torque ratios, the four individual torques on the wheels can be evaluated from the following equations:

$$T_{fl} = T\, r_{fr}\, r_{lr} \tag{3.3}$$

$$T_{fr} = T\, r_{fr}(1 - r_{lr}) \tag{3.4}$$

$$T_{rl} = T(1 - r_{fr})\, r_{lr} \tag{3.5}$$

$$T_{rr} = T(1 - r_{fr})(1 - r_{lr}) \tag{3.6}$$

Where T is the total torque on the vehicle.

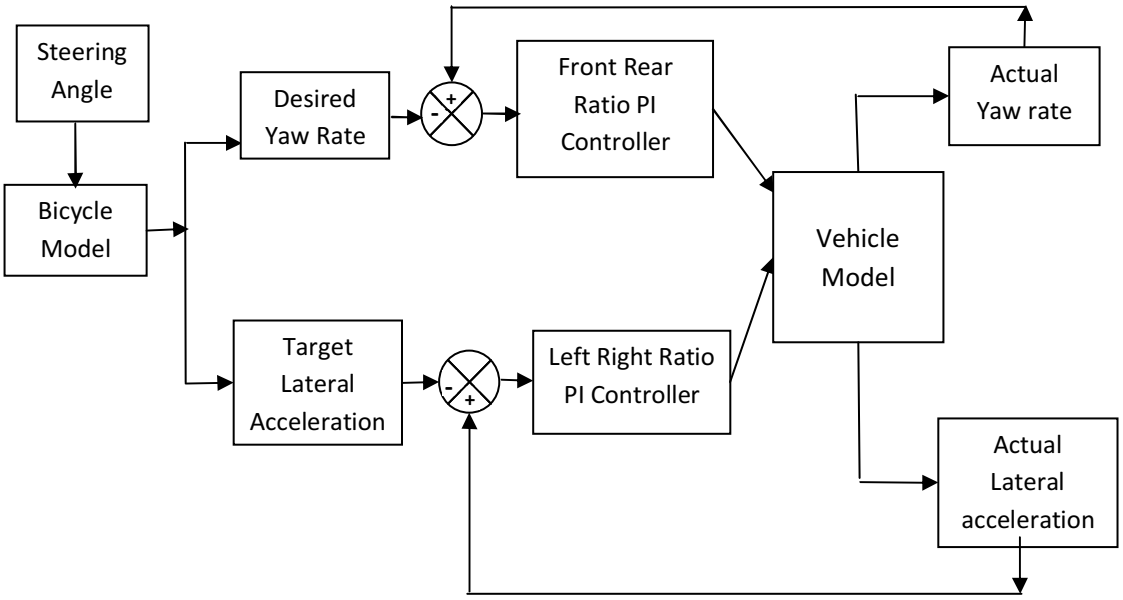


Figure 10 Torque Ratio Approach for VDC

The simulation results of the 'torque-ratio' approach described in (18) are encouraging in providing effective stability control. The variation in torques is constrained by the two ratios in this approach and the total torque on the vehicle always remains constant. Thus, this approach simplifies the control problem by reducing the control variables from four (each of four individual wheel torques) to two (two torque ratios) but reduces the freedom of torque distribution by imposing the constraints on total torque.

### 3.2.2 Approach II: Differential Torque Transfer

The other approach of torque distribution involves differential torque transfer i.e. addition or subtraction of corrective torques (the torque produced by upper controller of VDC system) to the individual wheel torques. This approach doesn't necessarily constrain the total torque to a constant value as is the case with Approach I described

above. This approach provides an additional degree of freedom in torque distribution thus allowing independent torque control of each wheel. In this study, this approach has been closely studied and implemented in simulations. The choice of appropriate feedback control variables (yaw rate and lateral acceleration) that go with this approach will be detailed in the next sub-sections.

Base Torque and Speed Control:

The torque distribution strategies are analyzed and implemented with and without controlling vehicle speed. In practice, various standard maneuvers are executed at constant or nearly constant speed. Considering this need, speed control (driver simulation) is introduced in some of the simulated tests. A simple PID function is used for the speed controller.

$$\Delta T_v = K_{p\_v} e_v + K_{i\_v} \int e_v dt + K_{d\_v} \frac{d}{dt}(e_v) \tag{3.7}$$

where the error function, $e_v$ ,is defined as the difference between the actual forward velocity, $v_x$ ,and the desired (set) forward velocity of the vehicle, $v_{x\_des}$.

$$e_v = v_x - v_{x\_des} \tag{3.8}$$

In general, in all simulations involving speed controlled (constant speed) maneuvers, the total torque $\Delta T_v$ is assumed to be equally distributed between all wheels. Accordingly, in the case of speed controlled VDC, the distributed (speed control) torque is added to the corrective torques produced by the VDC to each wheel. In the case of no speed control, constant torques termed as 'base torques' are provided to each wheel and

added to the corrective torques produced by VDC to each wheel. The total base torques on the left and right sides of the vehicle are given, respectively, by:

$$T_L = T_{fl} + T_{rl} \tag{3.9}$$

$$T_R = T_{fr} + T_{rr} \tag{3.10}$$

where $T_{fl}$, $T_{rl}$, $T_{fr,}$ $T_{rr}$ are the individual base torques acting on the individual wheels.

### 3.2.2.1 Yaw Rate Control

The difference between the actual yaw rate and the desired yaw rate is an obvious measure of deviation of the vehicle from its desired course and hence can be used to create the corrective yaw moment using an appropriate controller. In this work, the required differential torque, $\Delta T$ ,that would be added or subtracted to the base torques (in case of no speed control) or speed control torques of the individual wheels for generating the desired yaw moment, is evaluated from a PID type function of yaw rate error, $e_r$ and is given by:

$$\Delta T_r = K_{p1} e_r + K_{i1} \int e_r dt + K_{d1} \frac{d}{dt}(e_r) \tag{3.11}$$

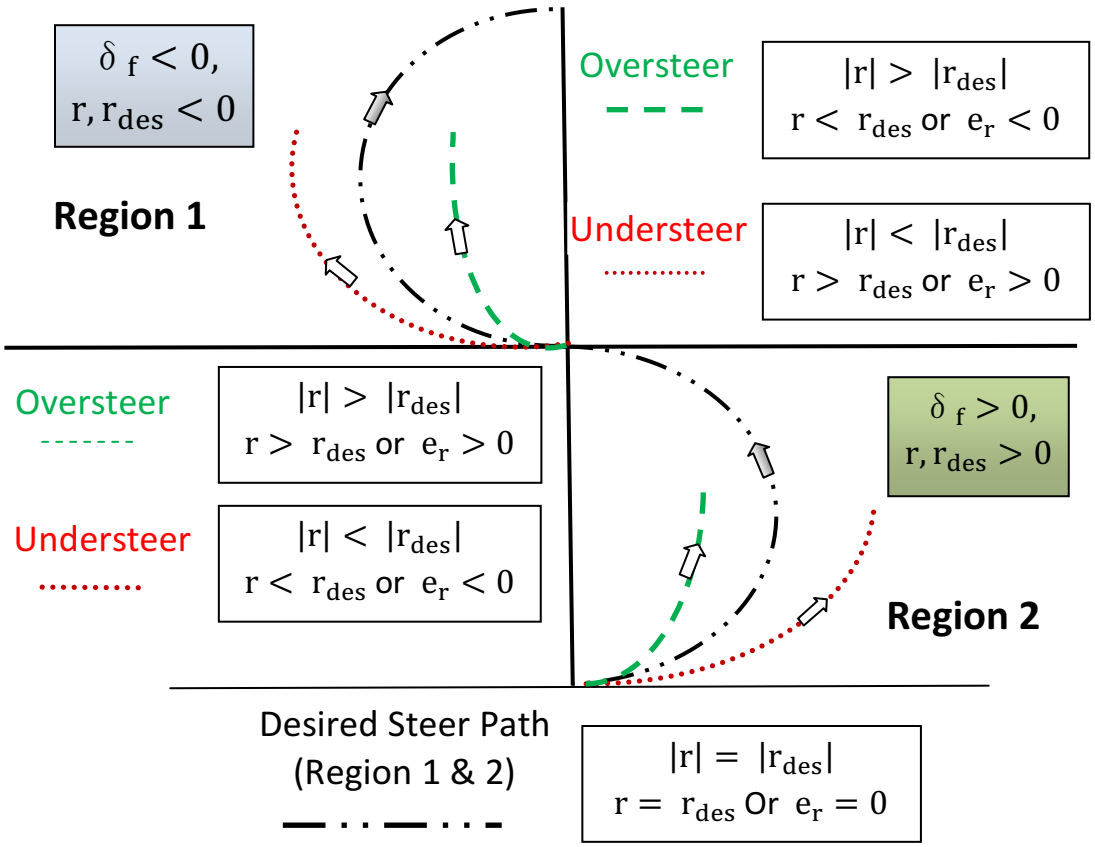


Figure 11 Schematic of Vehicle in Various Scenarios and Adopted Sign Conventions in Steady State

Let us consider the vehicle in different scenarios, including left or right hand turning and understeering or oversteering behavior. The conditions can be expressed mathematically for the two cases as follows.

**Case 1**: $\delta_f > 0$ or $r, r_{des} > 0$

For the left hand turn of the vehicle as shown in region 1 of Figure 11, the steering angle is positive. The desired and actual yaw rates are also positive as the per the sign convention adopted.

Oversteering occurs when $r > r_{des}$ or the yaw rate error, $e_r > 0$. and the vehicle understeers when $r < r_{des}$ or the yaw rate error, $e_r < 0$.

**Case 2**: $\delta_f < 0$ or $r, r_{des} < 0$

For the right hand turn of the vehicle as seen from region 2 of Figure 11, the steering angle is negative.

The vehicle oversteers when $|r| > |r_{des}|$ or $r < r_{des}$ , $e_r < 0$ . And understeering occurs when $r > r_{des}$ or the yaw rate error, $e_r > 0$.

For these scenarios, the following torque distribution strategies are conceived to achieve the corrective desired yaw moment. The strategies apply the torques to the left and right wheels of the vehicle, irrespective of direction of turn.

**Strategy 1**: Addition of corrective VDC torques only to left wheels

In this strategy, the corrective torques are applied only to left wheels while no corrective torques are applied to right wheels. That is:

$$T_{L\_new} = T_L + \Delta T_r \tag{3.12}$$

$$T_{R\_new} = T_R \tag{3.13}$$

The controller develops appropriate differential corrective torques in order to achieve desired corrective yaw moment and would be positive or negative depending on oversteering or understeering conditions:

$\Delta T_r > 0$ (Oversteering condition) (3.14)

$\Delta T_r < 0$ (Understeering condition) (3.15)

**Strategy 2**: Subtraction of corrective VDC torques only from right wheels

The drive torques on left wheels are unaltered while corrective torques are applied only to right wheels. That is:

$$T_{L_{new}} = T_L \tag{3.16}$$

$$T_{R\_new} = T_R - \Delta T_r \tag{3.17}$$

The differential corrective torques developed by the controller to generate the corrective yaw moment would be:

$\Delta T_r > 0$ (Oversteering condition)

$\Delta T_r < 0$ (Understeering condition)

**Strategy 3:** Switching corrective torque addition between left and right wheels

Yaw rate control torques are applied to the left or right part of the vehicle depending on the sign of the yaw rate error, $e_r$. For a positive yaw rate error (oversteering condition for left hand turn or understeering condition for right hand turn), the drive torques on the left wheels are increased while for a negative yaw rate error (understeering condition for left hand turn or oversteering condition for right hand turn), the drive torques on the right wheels are increased.

Mathematically, these are described as follows:

When $e_r > 0$ ,

$T_{L\_new} = T_L + |\Delta T_r|$

When $e_r < 0$ ,

$$T_{R\_new} = T_R + |\Delta T_r| \tag{3.18}$$

**Strategy 4**: Corrective VDC torques: add to left wheels and subtract from right wheels

In this strategy, half the corrective VDC torques are added to the left wheels and half of them are subtracted from the right wheels.

That is:

$$T_{L\_new} = T_L + \frac{\Delta T_r}{2} \tag{3.19}$$

$$T_{R\_new} = T_R - \frac{\Delta T_r}{2} \tag{3.20}$$

#### 3.2.2.2 Lateral Acceleration Control

With the lateral acceleration as the feedback variable, the required differential torque, $\Delta T_{a_y}$ can be evaluated from the PID type function of lateral acceleration error, $e_{a_y}$ in a similar way as was done in Section 3.2.1 for yaw rate control. This torque is given by:

$$\Delta T_{a_y} = K_{p2} e_{a_y} + K_{i2} \int e_{a_y} dt + K_{d2} \frac{d}{dt}\left(e_{a_y}\right) \tag{3.21}$$

The four strategies for torque distribution can be similarly applied as was done in Section 3.2.1 for yaw rate control. For example, a typical strategy (Strategy 4) can be expressed mathematically as:

$$T_{L\_new} = T_L + \frac{\Delta T_{a_y}}{2} \tag{3.22}$$

$$T_{R\_new} = T_R - \frac{\Delta T_{a_y}}{2} \tag{3.23}$$

#### 3.2.2.3 Combined Yaw Rate and Lateral Acceleration Control

This approach combines the Strategy 4 (corrective torques being added to left wheels and subtracted from right wheels) considering yaw rate error as well as lateral acceleration error. In so doing, this approach will also indirectly consider body side slip angle deviations. This can be easily understood from the mathematical expressions of lateral acceleration:.

$$a_y = \dot{v}_y + v_x * r \tag{3.25}$$

Recall that with smaller angle approximation, for small sideslip angles,

$$\tan\beta = \beta = \frac{v_y}{v_x} \tag{3.26}$$

Thus, equation 3.25 can be written as:

$$a_y = v_x * \dot{\beta} + \dot{v}_x * \beta + v_x * r \tag{3.27}$$

$$a_y \approx v_x * r + \dot{v}_x * \beta \tag{3.28}$$

The final wheel torques on the individual wheels can be given by:

$$T_{lf\_new} = T_{lf} + \frac{\Delta T_r}{2} + \frac{\Delta T_{a_y}}{2} \tag{3.29}$$

$$T_{lr\_new} = T_{lr} + \frac{\Delta T_r}{2} + \frac{\Delta T_{a_y}}{2} \tag{3.30}$$

$$T_{rf\_new} = T_{rf} - \frac{\Delta T_r}{2} - \frac{\Delta T_{a_y}}{2} \tag{3.31}$$

$$T_{rr\_new} = T_{rr} - \frac{\Delta T_r}{2} - \frac{\Delta T_{a_y}}{2} \tag{3.32}$$

## 3.3 Chapter Summary

This chapter detailed some Vehicle Dynamics Control systems and strategies which apply independent torque distribution management systems. Generation of the corrective yaw moment by front to rear torque transfer and side to side torque transfer was described with the physics- based explanation of variations in longitudinal forces achieved through torque transfer. Based on the physical consequence of longitudinal force distribution, two approaches of distribution of torque to each wheel of the vehicle were identified and explained.

The focus was on the proposed approach of differential torque transfer that provided an additional degree of freedom in torque distribution thereby allowing independent torque control of each wheel. Four torque distribution strategies for achieving the yaw moment control through each of the feedback control variables: yaw rate and lateral acceleration. The four strategies could also be applied a combined feedback of yaw rate and lateral acceleration for generating the desired corrective yaw moment.

# CHAPTER 4

# RESULTS AND DISCUSSIONS

In this chapter, simulation results will be presented from the different torque distribution strategies discussed in Chapter 3. The vehicle and tire data taken from a large front wheel drive saloon car, available in Appendix A of (16) , is used in the simulations.

It is to be recalled that the response of the basic vehicle dynamics model includes components due to the initial conditions of vehicle states, the steering input and the applied individual wheel torques. The presence or absence of a speed controller determines the base drive torques applied to each wheel; the speed controller is assumed independent of the VDC controller.

This chapter is organized as follows. The selection of suitable test maneuvers for analysis is discussed first in Section 4.1.

## 4.1 Selection of Test Maneuver

In order to analyze the effectiveness of the proposed VDC strategies, standard test maneuvers were considered and appropriately modified as explained in this section

### 4.1.1 Modified Fish-Hook Maneuver:

A standard fish-hook maneuver test designed by National Highway Traffic Safety Administration (NHTSA) for inducing and analyzing dynamic rollover (19)_has been reduced and modified appropriately to analyze the simulated VDC system. The modified fish hook maneuver, shown in Figure 12, includes the designed steer input to the system for the span of 10 sec. The maximum steer angle ($\pm$ A ) in deg and the slope of the ramp

(K) in deg/s in the standard maneuver (designed for rollover studies) have been reduced by the factor of 6.5 for simulating test conditions for the proposed analysis. First step in the simulation of this test maneuver involves calculation of the road wheel angle that produces 0.3 g of lateral acceleration. This is known as "Slowly Increasing Steer (SIS)". In the present case, it is calculated by equating the desired lateral acceleration, $a_{yd}$ to 0.3 g's and longitudinal velocity, $v_x$ to 80 kmph. Thus, SIS = 3.8 deg of road wheel angle (denoted by 'A' in Figure 12)

The maximum steer angle for the fish-hook maneuver is set at SIS, with a ramp speed of K = (720/6.5) deg/s. At the desired test speed ($v_x$ = 80 kmph), the vehicle is quickly ramped to this angle (A). It's held for just 0.25 sec and is suddenly ramped to the opposite steer limit(-A) and held for 3 sec before the vehicle is ramped back to zero steer (straight-ahead) position as shown in Figure 12.

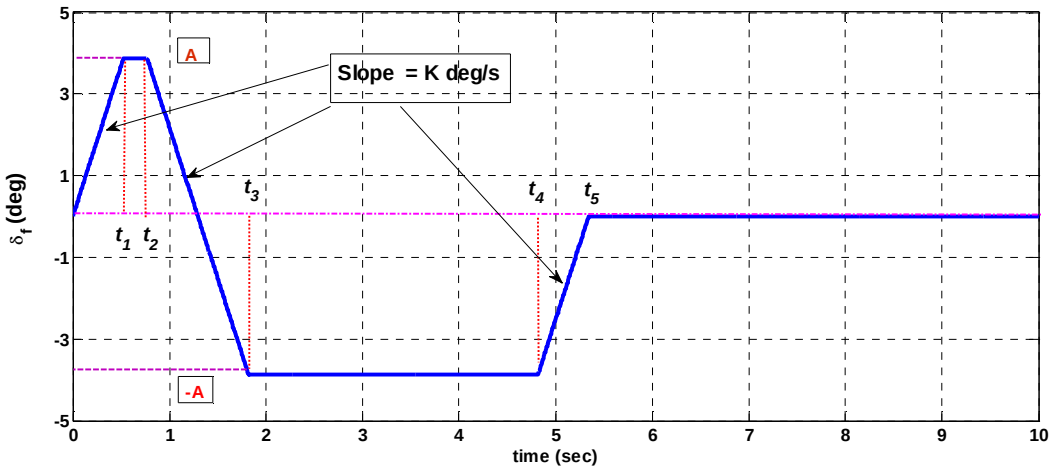


Figure 12 Modified NHTSA Fish hook Maneuver Test Input

#### 4.1.2 FMVSS 126 ESC Test Maneuver:

The Federal Motor Vehicle Safety Standard (FMVSS) No. 126 test for electronic stability control systems (20) has been modified suitably and implemented for evaluating the performance of proposed VDC strategies.

In this test, a “Slowly Increasing Steer” angle is first defined as the average steering wheel angle (road wheel angle) associated with a lateral acceleration of the vehicle mass center at 0.3 g. This is determined in a similar way as was done for fish-hook maneuver (Section 4.1.1). That steering wheel angle is designated **A** and is used to define and evaluate the test that follows. The test includes a "Sine with Dwell" test conducted with "a steering pattern of a sine wave at 0.7 Hz frequency with a 400 ms delay beginning at the second peak amplitude" (see Figure 13).

The original standard FMVSS 126 ESC test requires three sets of tests. It increments the steering angle (Slowly Increasing Steer angle) based on the logic that involves driver model and checking of the defined vehicle states at up to three times during the run to decide the success or failure of each of the tests in the series (20).

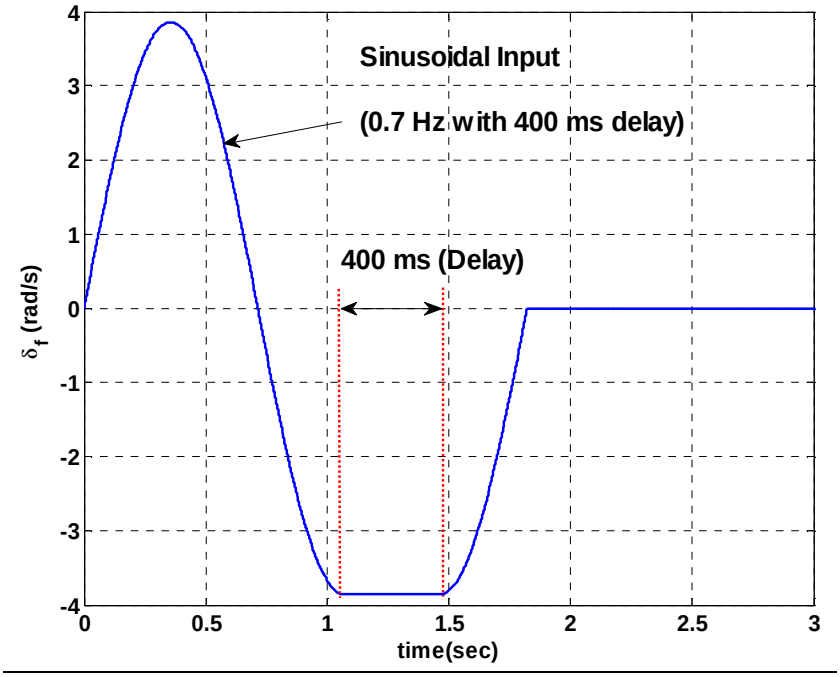


Figure 13 FMVSS 126 VDC Test Steer Input

### 4.1.3 J-turn (Step Steer)

A standard J-turn test is conducted to study the performance characteristics of a VDC system like its tracking ability in a sudden steer angle change (step steer). A typical step steer profile of road wheel angle (RWA) with the step applied at 1$^{st}$ sec and achieving the required road-wheel angle in 0.1 sec (ramp with the slope of 30 deg/s) is shown in Figure 14.

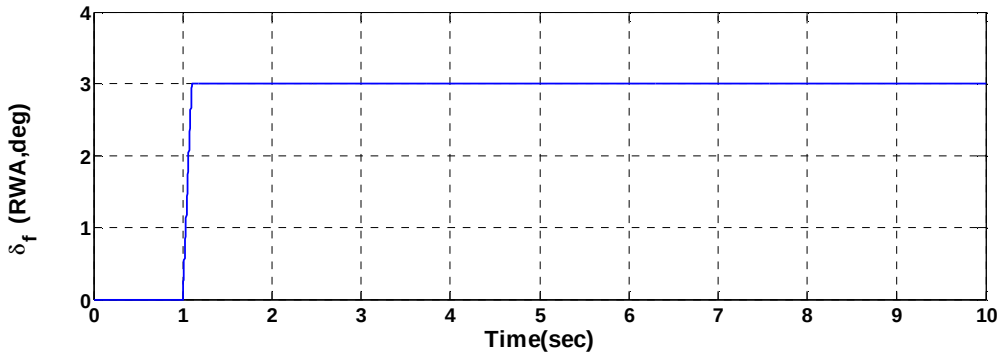


Figure 14 Step Steer Input for RWA = 3 deg

## 4.2 Simulation of Road Surface conditions

Different road surface conditions (different coefficients of friction between road and tires, μ) were simulated to evaluate the effectiveness of proposed VDC strategies. Dry Surface (μ = 1), wet surface (μ = 0.6) and very slippery surface (μ = 0.3) were simulated using corresponding friction scaling factors in the Pacejka Tire model (21).

## 4.3 Yaw Rate Control

The torque distribution strategies developed with yaw rate control (as explained in Section 3.2.2.1) were simulated for different road conditions, steering inputs and controller gains and for cases with and without speed control (the simulation of speed control by the driver).

### 4.3.1 VDC: Torque Distribution Strategy 4

The VDC torque distribution strategy 4 (addition of VDC corrective torques to left wheels and subtraction from right wheels) has been implemented on dry surface (μ = 1) with the fish-hook steering input described in Section 4.1.1.

Figure 15 and Figure 16 show the time history plot for the yaw rate controller. They clearly show that the yaw rate controller has been very effective in tracking of the yaw rate and lateral acceleration of the vehicle. Sideslip angle of the vehicle remains very small and always below the steady state values computed from bicycle model as shown in Figure 17.This renders separate β - control unnecessary for this test case and test vehicle.

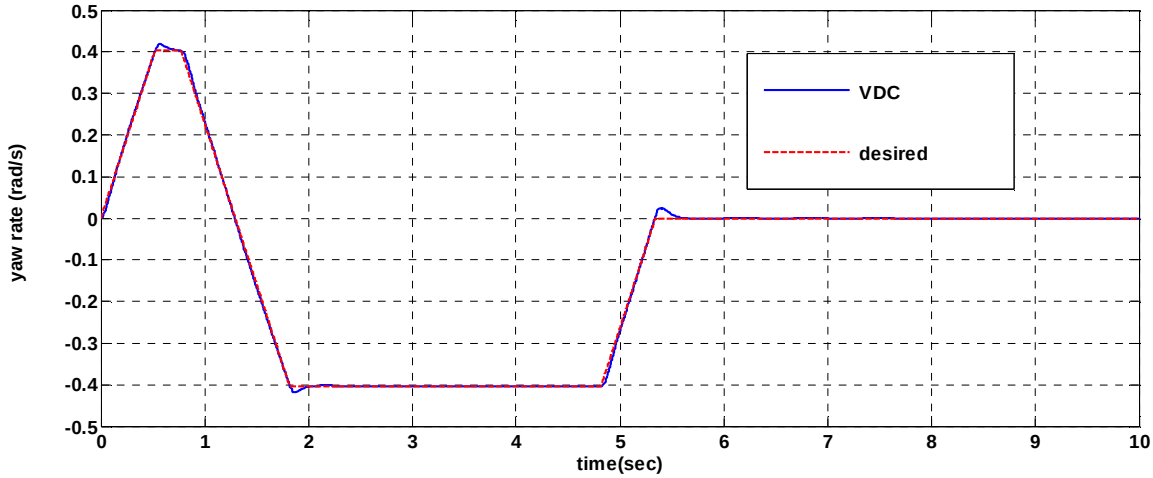


Figure 15 Yaw Rate Time History Plot (VDC Controlled System Vs. Desired) Torque Distribution Strategy 4 with Speed Control: Dry surface (μ = 1)

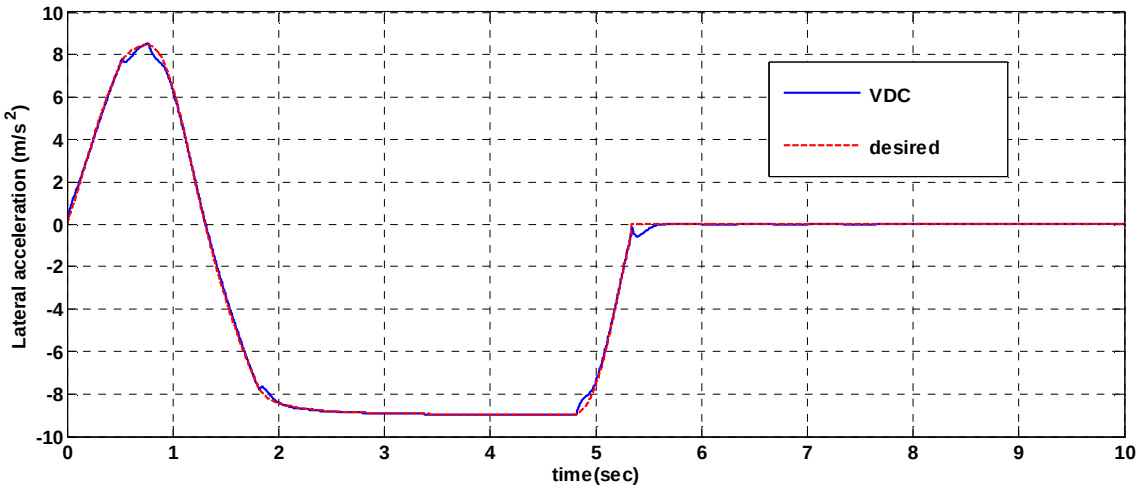


Figure 16 Lateral Acceleration Vs. Time (VDC Controlled System Vs. Desired) Torque Distribution Strategy 4 with Speed Control: Dry surface (μ = 1)

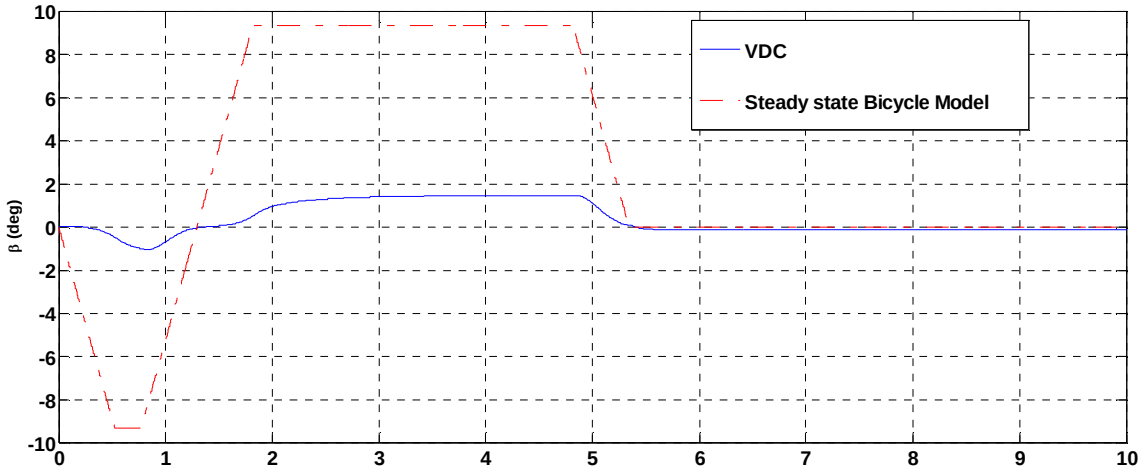


Figure 17 Vehicle Sideslip Angle Vs. Time (VDC Controlled System Vs. Desired)Torque Distribution Strategy 4 with Speed Control: Dry surface ($\mu = 1$)

The control effort for this yaw-rate based VDC controller can be measured by looking at the torques at each wheel. Input torques to front left wheels are shown in Figure 18. The controller reaches peak torque levels during the times of peak steer and return zero steer (straight-line motion) of the maneuver. It can be seen that to achieve this level of yaw rate correction (for the controller gains selected, and response tracking achieved as shown above), the yaw rate controller exerts driving torque on left part of the vehicle (front and rear wheels) which indicated by positive torque peaks while applying significant braking torque on the right side (both, front and rear wheels) which is indicated by negative torque peaks in the plots shown in Figure 18.

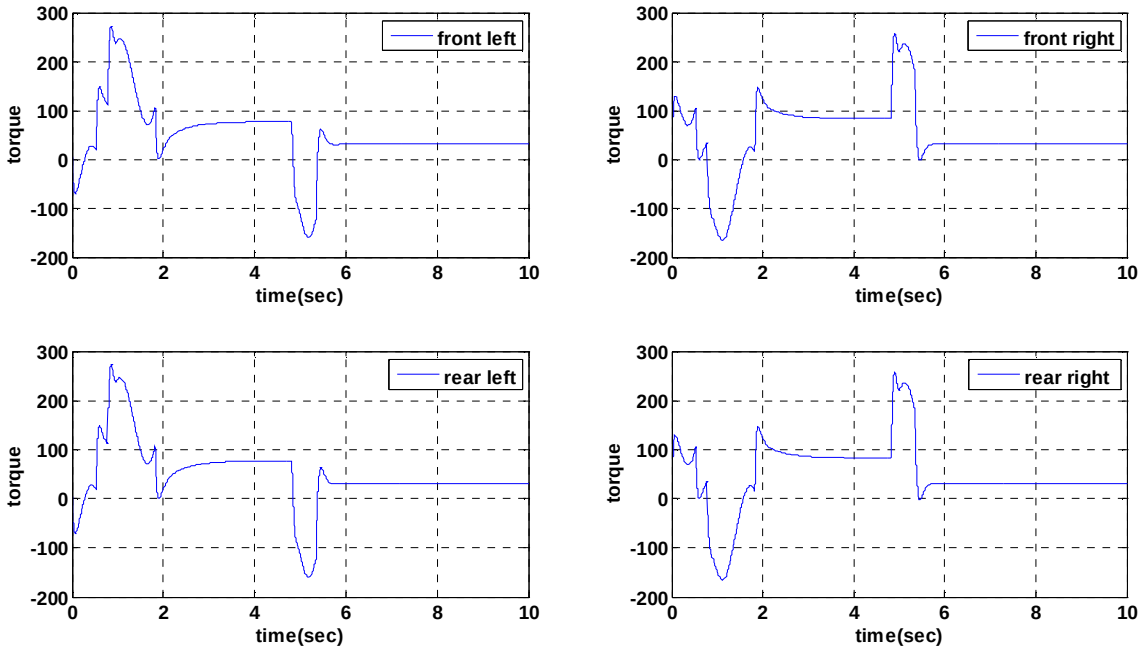


Figure 18 Individual Final Wheel Torques of VDC Controlled Vehicle Torque Distribution Strategy 4 with Speed Control: Dry surface (μ = 1)

Figure 19 gives the plots of individual longitudinal wheel slip ratios with time corresponding to the control strategy presented above. Peak slip ratio values can be attributed to the peak values of corresponding individual wheel torques exerted for achieving required yaw correction. These slip values still remain in the linear region of $F_x$ vs.- Slip ratio curve and the wheels and don't show any tendency to lock or spin. Hence, additional slip control is not required in this particular scenario.

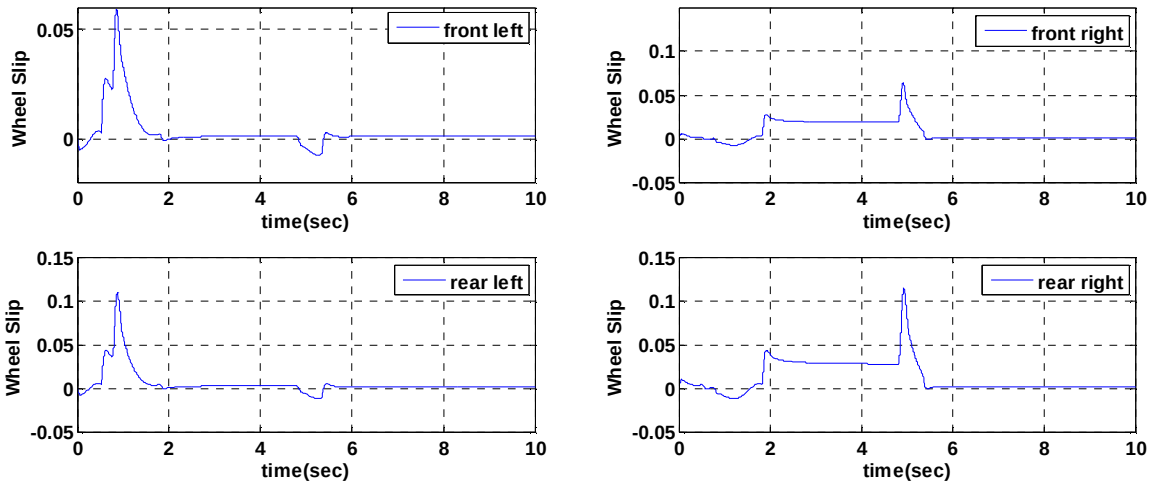


Figure 19 Individual Wheel Slips (VDC: Yaw Control) Torque Distribution Strategy 4 with Speed Control: Dry surface (μ = 1)

### 4.3.2 Effect of VDC and Speed Control

The vehicle performance parameters, yaw rate and lateral acceleration are compared for the vehicle with and without VDC in the presence or absence of speed controller (the driver simulation of vehicle speed control at 80 kmph). The torque distribution Strategy 4 is implemented on the vehicle with VDC on dry surface conditions (μ = 1) using the steering input obtained from FMVSS 126 ESC test described in Section 4.1.2.

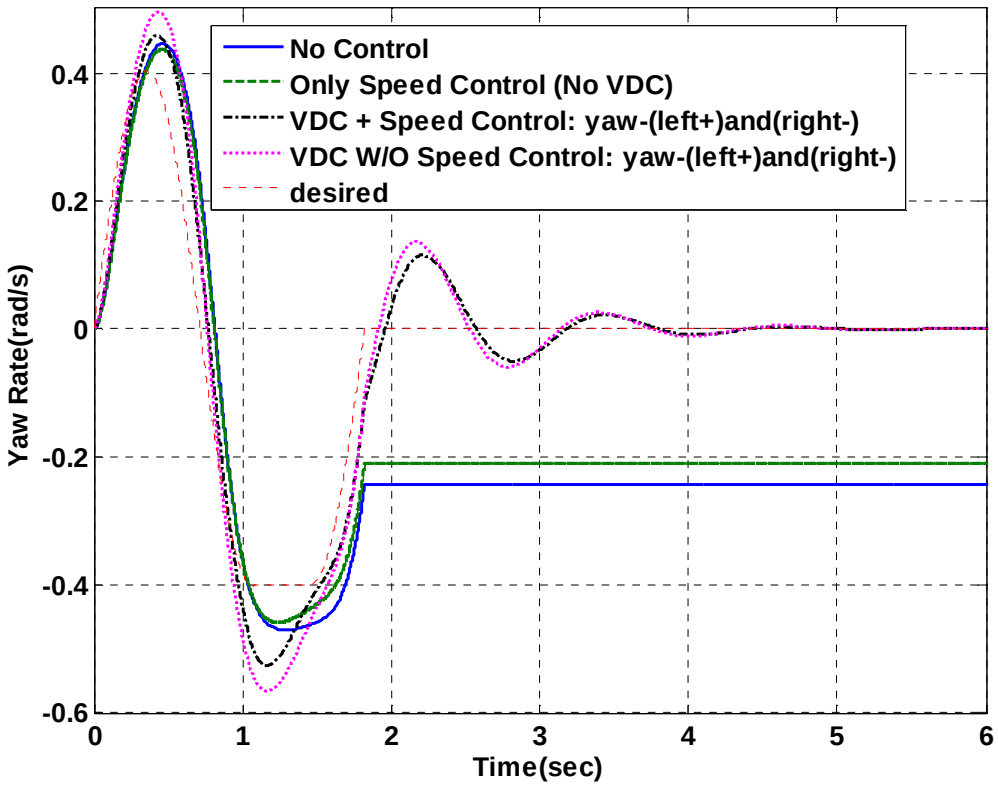


Figure 20 Yaw Rate Response (VDC Controlled and Uncontrolled) Torque Distribution Strategy 4: Dry surface ($\mu = 1$)

The time history plot of the yaw rate response (Figure 20) clearly shows that a speed controlled VDC is able to return to zero steer motion (straight-line motion) and maintain it while the uncontrolled system cannot. The VDC controlled system tracks the desired yaw rate closely.

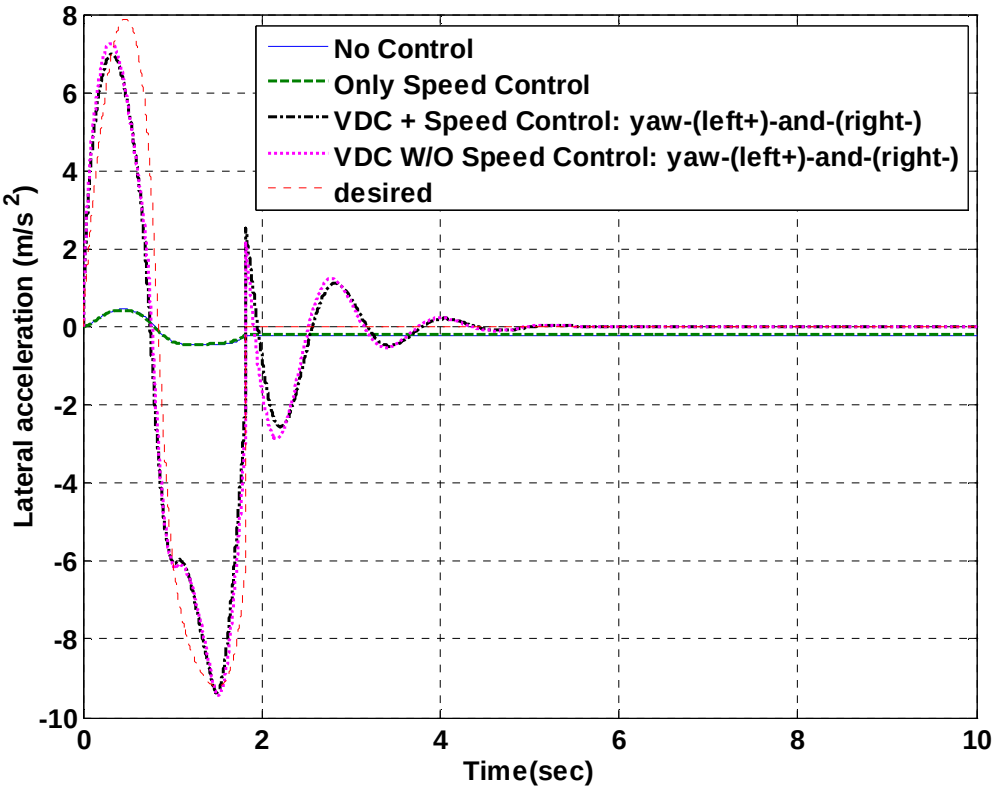


Figure 21 Lateral Acceleration Response (VDC Controlled and Uncontrolled) Torque Distribution Strategy 4 with Speed Control: Dry surface ($\mu = 1$)

The time history plot of lateral acceleration (Figure 21) shows that a speed controlled VDC can track the desired values while the uncontrolled system can't reach higher desired values.

### 4.3.3 VDC For Sudden Changes In Steering Input (J-Turn)

To study the tracking ability of the system for sudden changes in steering angle, the performance of the vehicle with VDC in presence of speed controller (driver simulation) and uncontrolled vehicle is compared. The torque distribution Strategy 4 is implemented on the vehicle with VDC on dry surface conditions ($\mu = 1$) using the steering input of 3 deg RWA (road wheel angle) obtained from J-turn (step steer) test described in Section 4.1.3. The time history plots of yaw rate, lateral acceleration and sideslip angle for first 6 sec are shown in Figure 22, 23 and 24.The sudden change in steering angle causes the overshoot at 1.1 sec for selected set of higher controller gains as seen in all the plots. The oscillations settle down quickly and good tracking ability for yaw rate and lateral acceleration responses is observed. The sideslip angle remains very small.

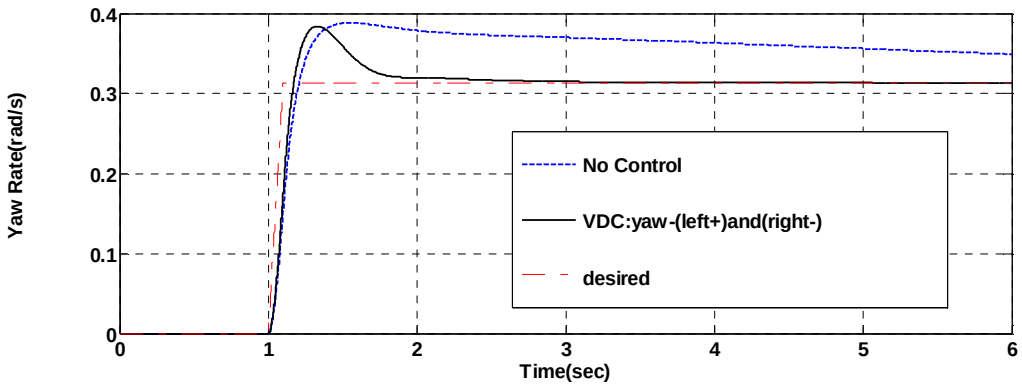


Figure 22 Yaw Rate Response to Step Steer of 3 deg RWA(VDC Controlled and Uncontrolled) Torque Distribution Strategy 4 with Speed Control: Dry surface ($\mu = 1$)

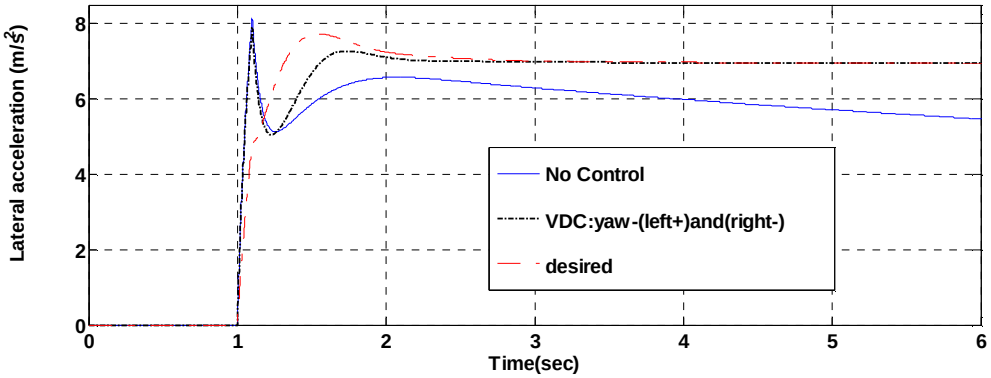


Figure 23 Lateral Acceleration Response to Step Steer of 3 deg RWA (VDC Controlled and Uncontrolled) Torque Distribution Strategy 4 with Speed Control: Dry surface (μ = 1)

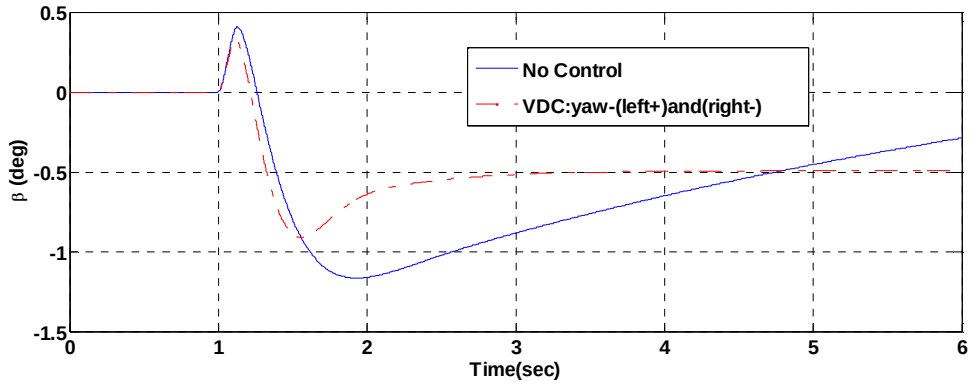


Figure 24 Sideslip angle Response to Step Steer of 3 deg RWA (VDC Controlled and Uncontrolled) Torque Distribution Strategy 4 with Speed Control: Dry surface (μ = 1)

### 4.3.4 Effect of Controller Gains on Performance:

Three sets of PID Controller gains were used for comparative study of the effect of controller strengths on vehicle performance. Figure 25 shows the yaw rate of the vehicle in each case against the desired output. We can observe the improvement in the tracking ability and faster return to the straight-line motion with increasing controller gains. The resulting torques at the front left wheel are shown in Figure 26.

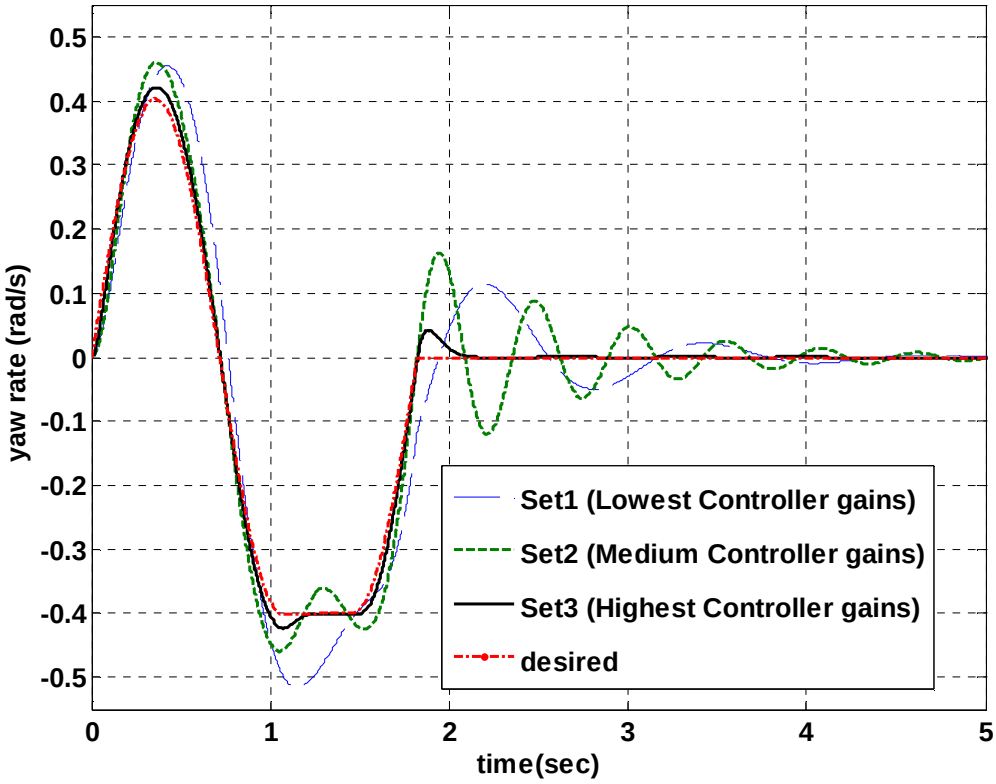


Figure 25 Yaw Rate Response: Comparison of Controller Gains (Yaw Rate Error Feedback: Dry surface ($\mu = 1$))

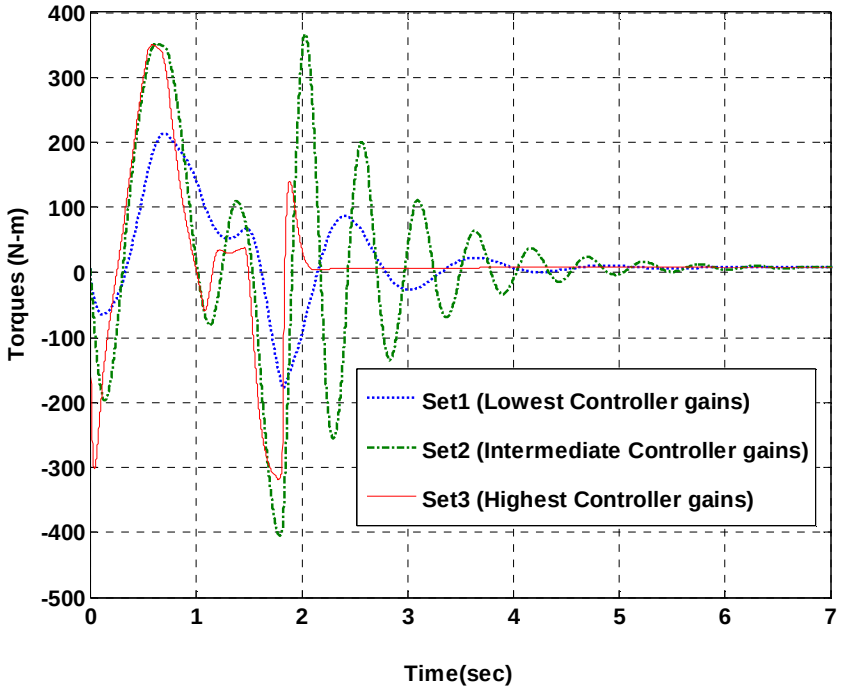


Figure 26 Torques on Front left Wheel: Comparison of Controller Gains (Yaw Rate Error Feedback: Dry surface ($\mu = 1$))

Table 1 gives the values of the actual controller gains used and a brief summary of the effect of controller gains on vehicle performance.

Table 1 Vehicle Performance for Different Controller Strengths: Yaw Rate Error Feedback

| | Set 1 (lowest gains) $K_P$ = 1000, $K_I$ = 1000, $K_D$ = 0 | Set 2 (medium gains) $K_P$ = 1000, $K_I$ = 10000, $K_D$ = 0 | Set 3 (highest gains) $K_P$ = 1000, $K_I$= 100000, $K_D$ = 0 |
|---|---|---|---|
| Yaw rate tracking ability (deviation error ,$e_{tr}$ in $rad^2/s^2$) | 17.0551 | 11.4607 | 0.7107 |
| Oscillations (End of maneuver) | | | |
| Maximum overshoot | 0.115 | 0.165 | 0.042 |
| Settling time | 2.7 | 2.7 | 0.3 |
| Controller effort required(Torques on front left wheels ) (Max. Torque, Min. Torque in Nm) | 214,-180 | 352,-400 | 352,-320 |

### 4.3.5 Comparison of Torque Distribution Strategies

To compare the different yaw-control strategies discussed in Chapter 3, simulations were carried out with steering input designed according to FMVSS 126 test maneuver described before. Set1 of controller gains (the lowest set) giving with the slowest responses was taken to more clearly make out the differences in the results for the different strategies. The simulation results on dry surface ($\mu = 1$) with and without speed control are discussed in the next sub-sections:

#### 4.3.5.1 VDC with Speed Control

It is to be noted again that the desired speed of 80 kmph is maintained on dry surface ($\mu = 1$) using the speed controller during implementation of different yaw-control strategies.

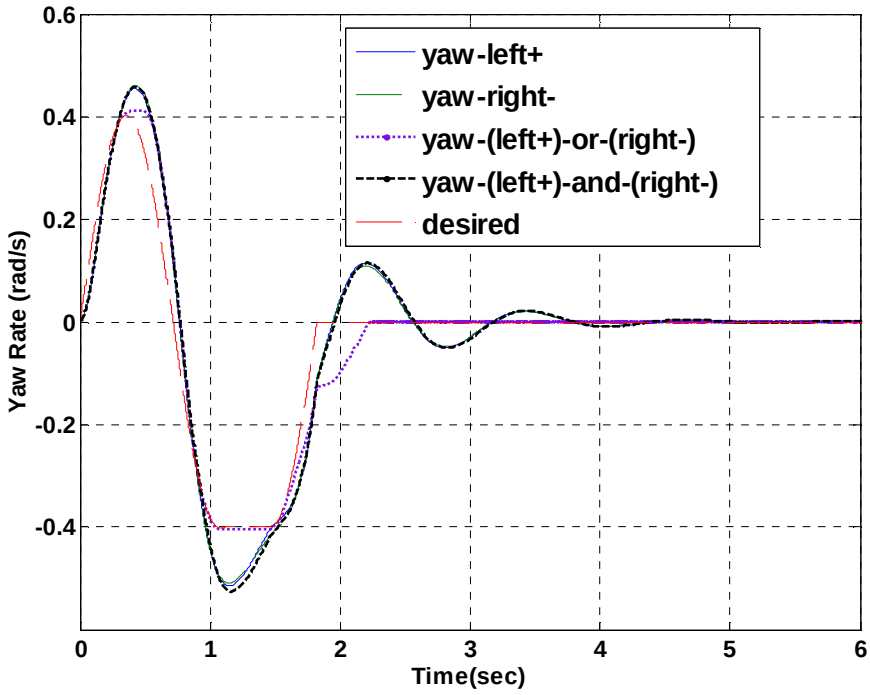


Figure 27 Yaw Rate Response: Comparison of VDC Strategies (Yaw Rate Error Feedback with Speed Control: Dry surface ($\mu = 1$))

Figure 27 shows the comparison of yaw rate responses for all control strategies along with the response from the respective VDC. Strategy 1, 2 and 4 show quite similar time history plots while strategy 3 gives much better results than all of them in terms of tracking ability and oscillating behavior. The vehicle returns to its straight-line motion very fast without any oscillations.

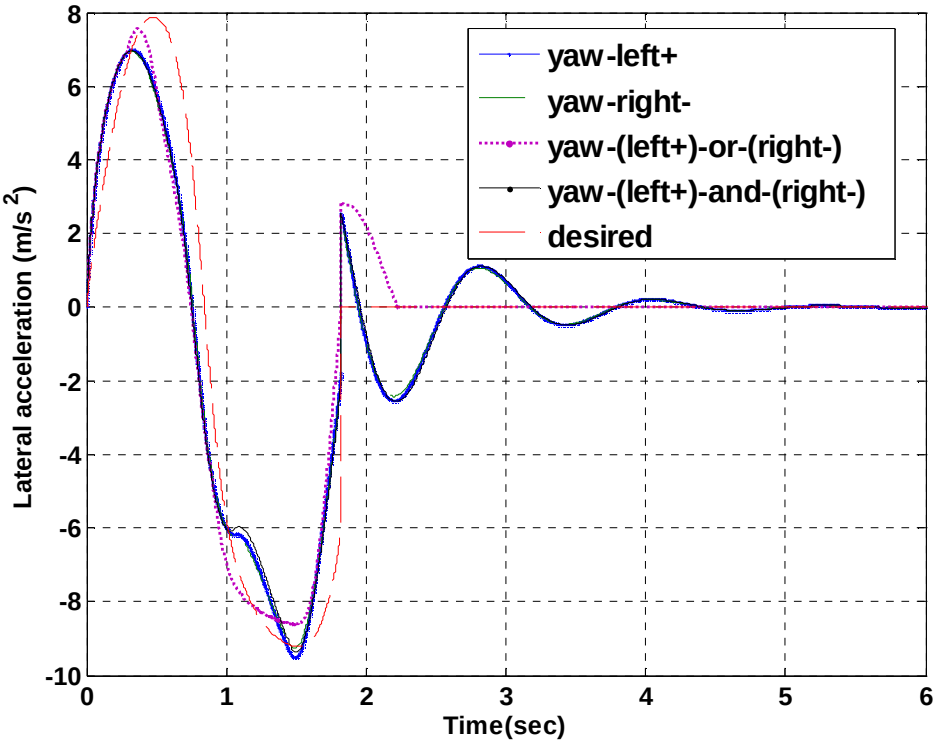


Figure 28 Lateral Acceleration Response: Comparison of VDC Strategies (Yaw Rate Error Feedback with Speed Control: Dry surface ($\mu = 1$)))

Figure 28 explains similar comparisons for lateral acceleration rate response as observed in Figure 27. Strategy 3 shows higher overshoot at the end of maneuver but settles down quickly.

In order to compare the control effort required by each control strategy, input torques to front left wheels in each case are plotted as shown in Figure 29. It can be seen that the

maximum torque required is highest for strategy 2 amongst all, while strategy 1 requires a lower maximum torque and the lowest straight-line torque (torque required to maintain the straight-line return motion). Strategy 3 shows high fluctuations in torques as this strategy involves a switch that selects the torque distribution strategy employed in strategy 1 or 2 based on yaw rate error function. This gives it properties of a variable structure controller, which is known to lead to control chatter for choices of high gain.

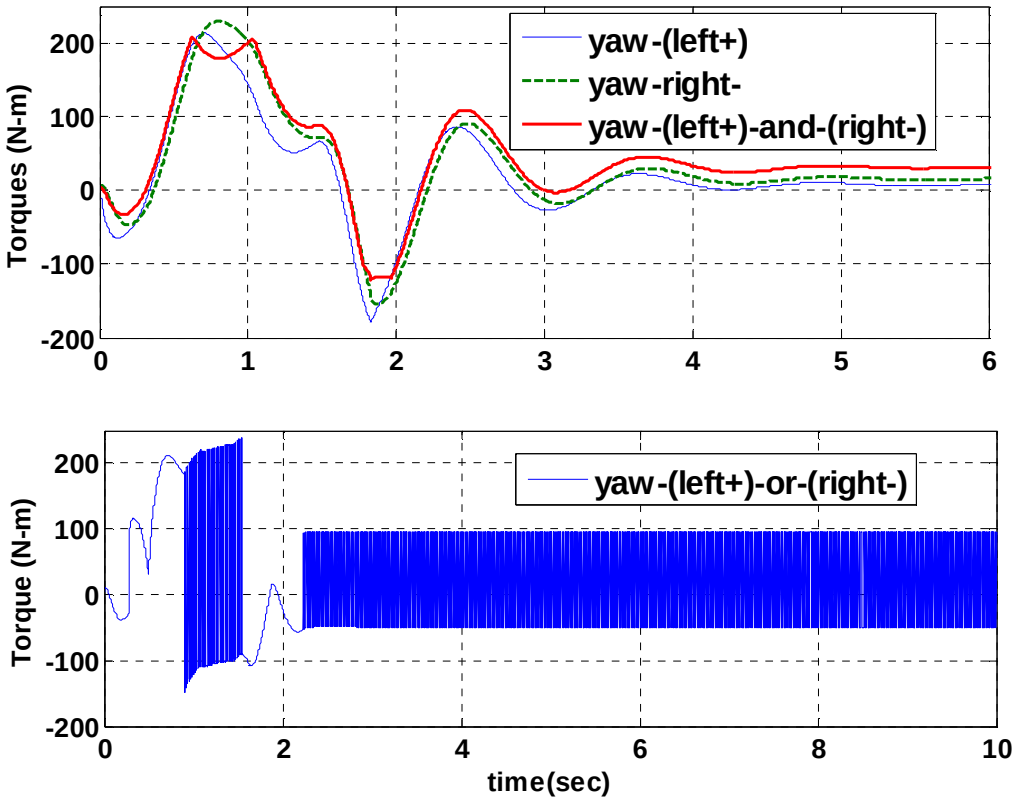


Figure 29 Torques on Front left Wheel: Comparison of VDC Strategies (Yaw Rate Error Feedback with Speed Control: Dry surface ($\mu = 1$)))

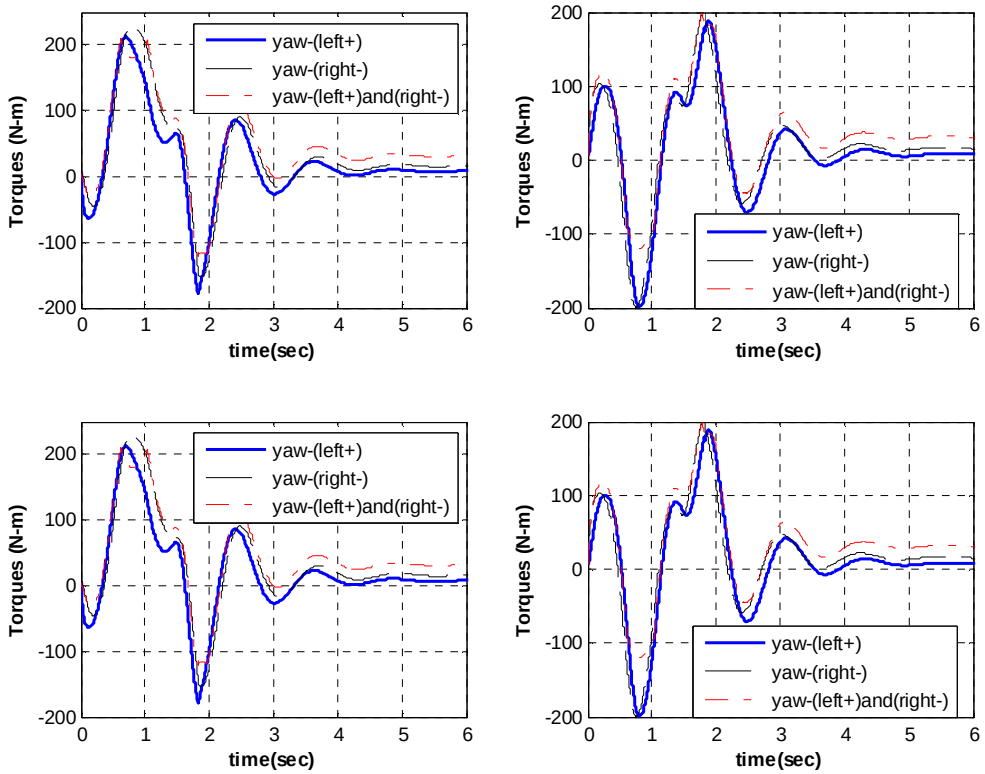


Figure 30 Final Torques on individual wheels: Comparison of VDC Strategies (Yaw Rate Error Feedback with Speed Control: Dry surface (μ = 1)))

It should be recalled from Chapter 3 that the corrective yaw moment torques are added only to inner wheels for strategy 1 while they are subtracted only from outer wheels in case of strategy 2. But as observed from Figure 30, the time history plots of the final torques corresponding to both of these strategies in case of each wheel are close and overlapping during most of the time. This can be explained as follows. The torques developed by speed controller are such that when the yaw rate controller corresponding to strategy 1 adds positive torques to the left wheels of the vehicle , the overall torque on the vehicle increases and hence the vehicle speed. The speed controller develops negative

torques and adds equally to the corrective yaw torques on all the wheels, thus the net torques on outer wheels are negative while those on inner wheels are positive but reduced accordingly. The variations in the torques on individual wheels corresponding to strategy 2 can be explained similarly.

To further distinguish between these strategies more clearly, speed controller is switched OFF and the simulations were carried out, the results of which are explained in the next subsection.

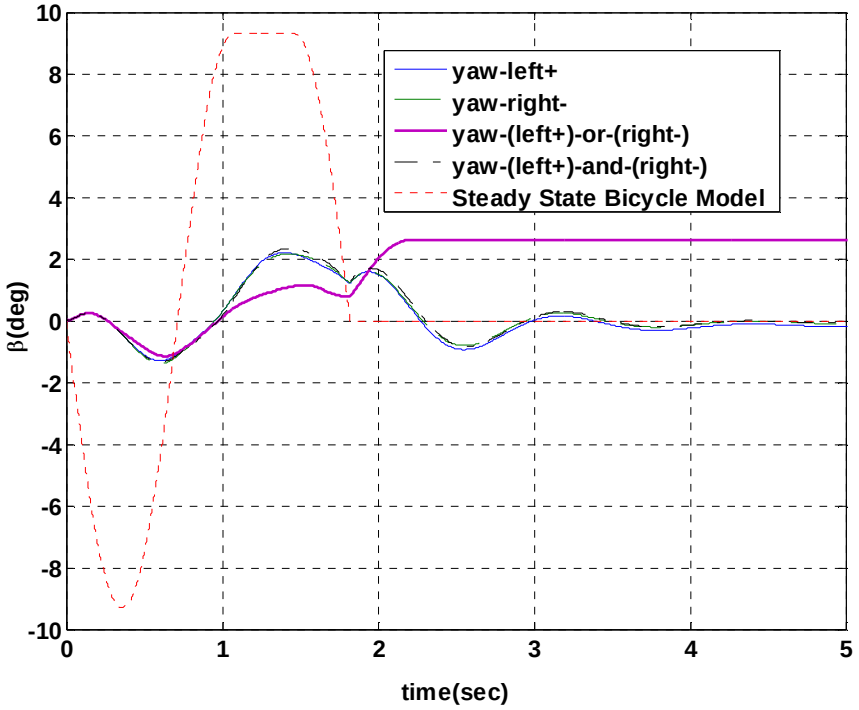


Figure 31 Sideslip Angle Response: Comparison of VDC Strategies (Yaw Rate Error Feedback with Speed Control: Dry surface ($\mu = 1$)))

Figure 31 shows quite interesting results for the side angle response under yaw-rate control. Sideslip angle values are even less than the steady state values obtained from the

bicycle model of the vehicle during the maneuver. The yaw rate control, in these test cases, had the added benefit of keeping the side slip angle β small.

Table 2 gives the summary of comparative study of the four torque distribution strategies for yaw rate control. Different performance evaluation parameters are defined in terms of deviation errors and numerical values for quantitative comparisons of outputs with the strategies.

Table 2 Comparison of VDC Strategies: Yaw Rate Error Feedback

| Performance Evaluation Parameter | Strategy 1 | Strategy 2 | Strategy 3 | Strategy 4 |
|---|---|---|---|---|
| Yaw rate tracking ability (deviation error , $e_{tr}$ in $rad^2/s^2$) | 17.0551 | 17.0113 | 10.5320 | 18.6099 |
| Lateral acceleration tracking ability (deviation error ,$e_{tay}$ in $m^2/s^4$) | 10016 | 9392 | 10714 | 1022.1 |
| Oscillations (End of maneuver) | | | | |
| Max overshoot | 0.1145 | 0.109 | No overshoot | 0.115 |
| Settling time (sec) | @ 3 | @ 3 | @0.5 | @ 3 |
| Controller effort for (Max.Torque, Min.Torque in Nm) | 213,-180 | 230,-154 | 240,-150 | 210,-120 |

#### 4.3.5.2 VDC without Speed Control

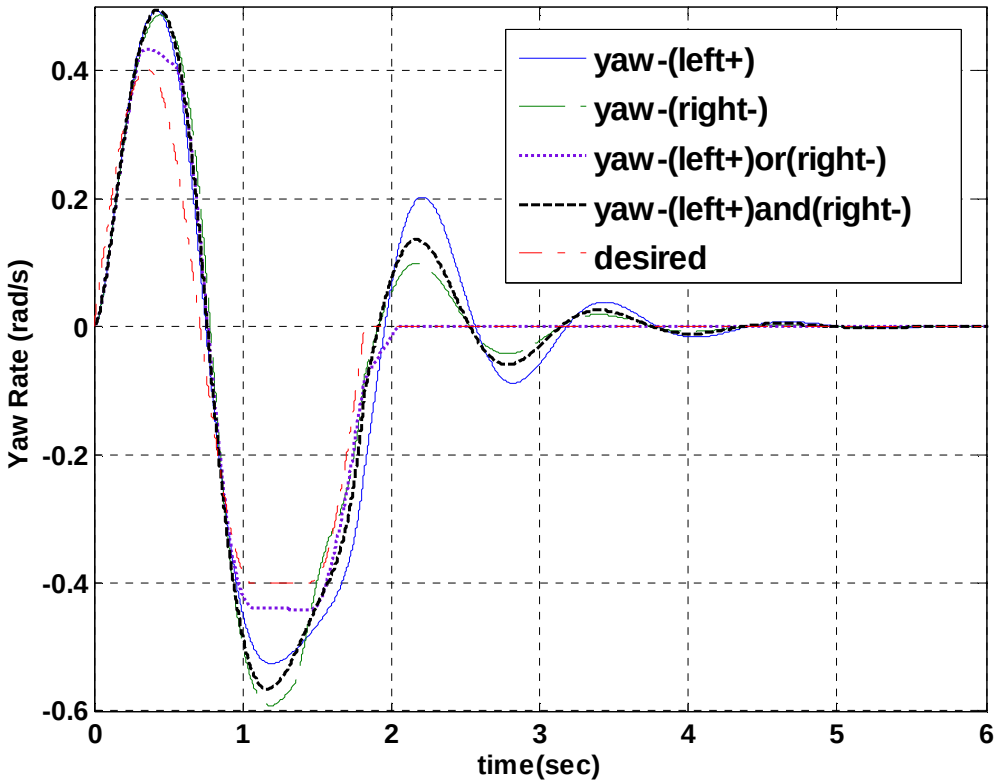


Figure 32 Yaw Rate Response: Comparison of VDC Strategies (Yaw Rate Error Feedback with No speed control: Dry surface ($\mu = 1$)))

With the speed controller switched OFF, the resultant final wheel torques corresponding to each of strategies 1 and 2, on one set of wheels (right wheels in case of Strategy1 or left wheels in case of Strategy 2) are constant as shown in Figure 32.

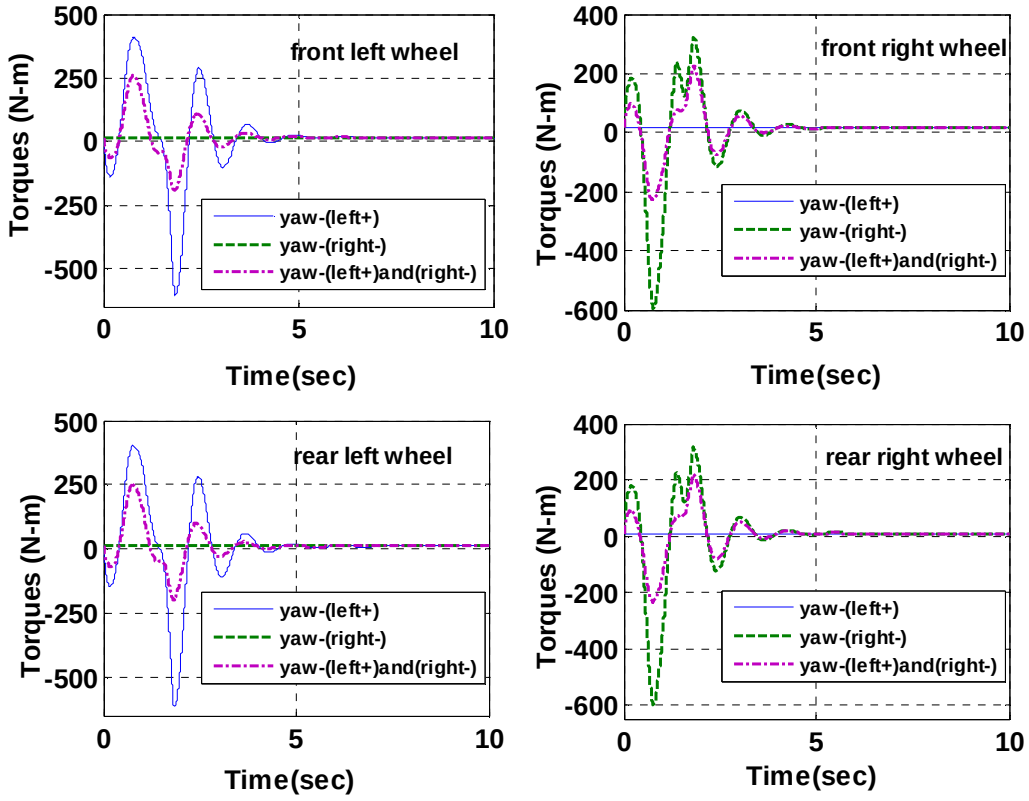


Figure 33 Resultant Torques on Individual Wheels: Comparison of VDC Strategies (Yaw Rate Error Feedback with No speed control: Dry surface (μ = 1)))

## 4.4 Lateral Acceleration Control

Lateral acceleration control (as explained in Section 3.2.2.2) was implemented on a slippery surface (low-coefficient of friction, μ = 0.3) with and without speed control.

Figure 33, 34, 35 and 36 show the results achieved by this control using torque distribution Strategy 4 with the vehicle speed being maintained at 40 kmph.

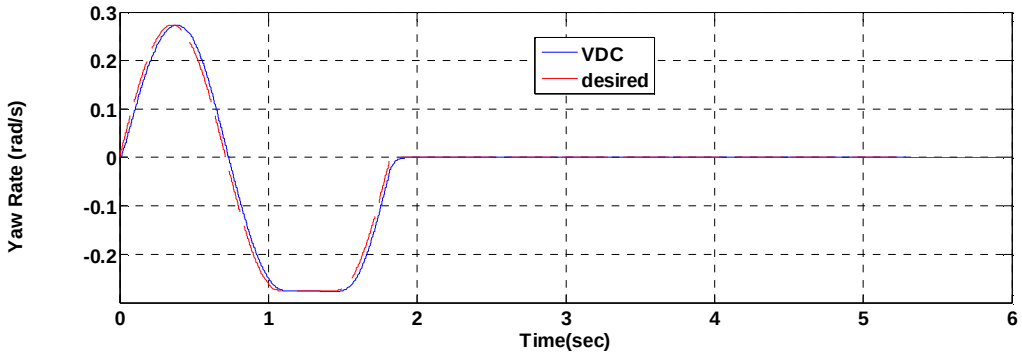


Figure 34 Yaw Rate Response (Lateral Acceleration Error Feedback with Speed Control on Slippery surface (μ = 0.3))

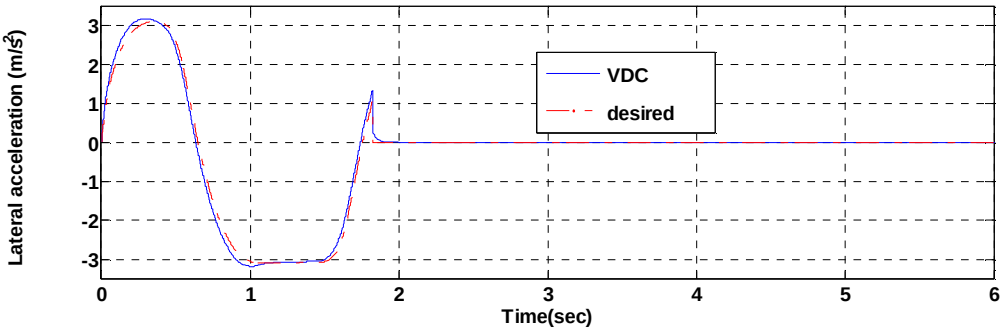


Figure 35 Lateral Acceleration Response (Lateral Acceleration Error Feedback with Speed Control on Slippery surface (μ = 0.3))

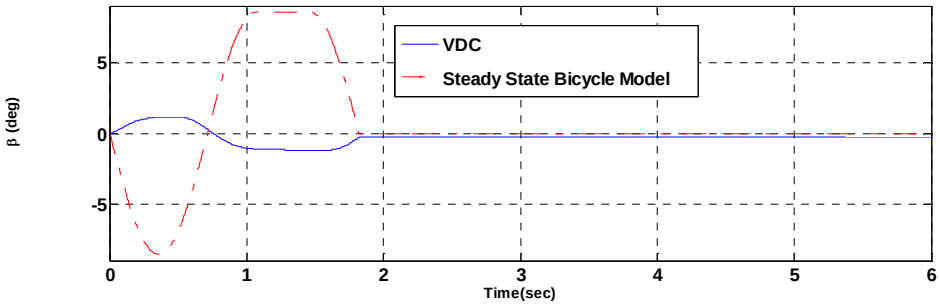


Figure 36 Sideslip Angle Response (Lateral Acceleration Error Feedback with Speed Control on Slippery surface (μ = 0.3))

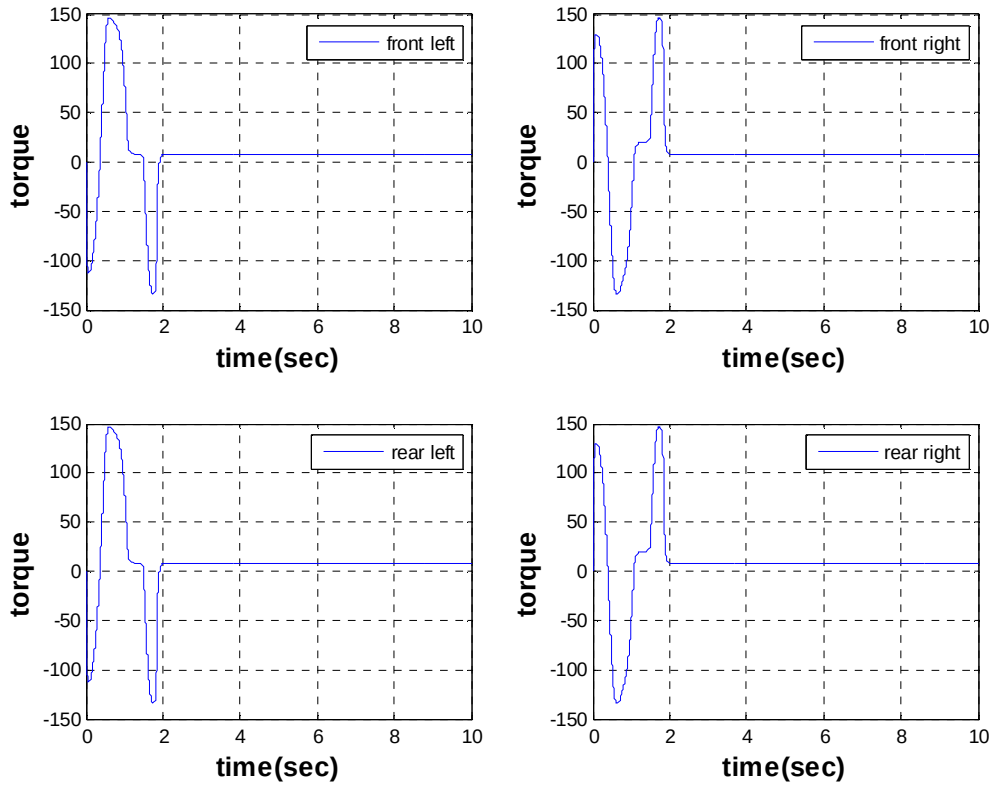


Figure 37 Resultant Torques on Individual Wheels (Lateral Acceleration Error Feedback with Speed Control on Slippery surface (μ = 0.3))

## 4.5 Combined Control (Feedback Control Using Yaw Rate and Lateral Acceleration both)

Combined control (Feedback Control using Yaw Rate and Lateral Acceleration, both) was implemented on a slippery surface (low-coefficient of friction, μ = 0.3) with speed control. Figure 37, 38, 39 and 40 show the results achieved by this control using torque distribution Strategy 4 with the vehicle speed being maintained at 50 kmph.

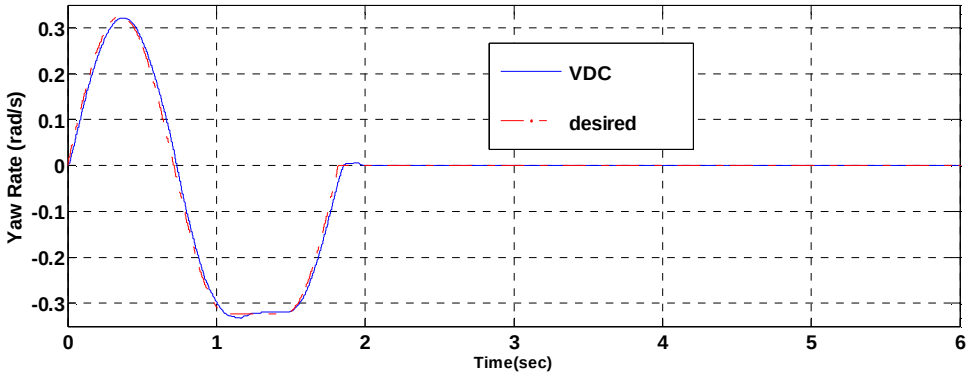


Figure 38 Yaw Rate Response (Combined (Yaw Rate and Lat. Acc.) Error Feedback with Speed Control on Slippery surface (μ = 0.3))

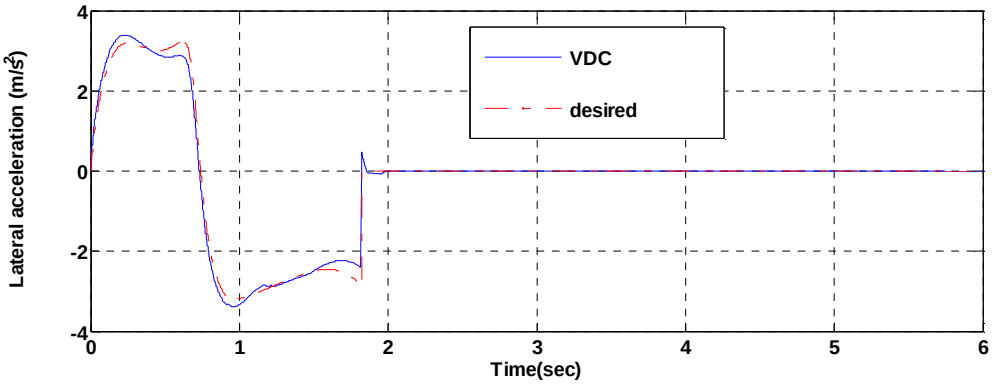


Figure 39 Lateral Acceleration Response (Combined (Yaw Rate and Lat. Acc.) Error Feedback with Speed Control on Slippery surface (μ = 0.3))

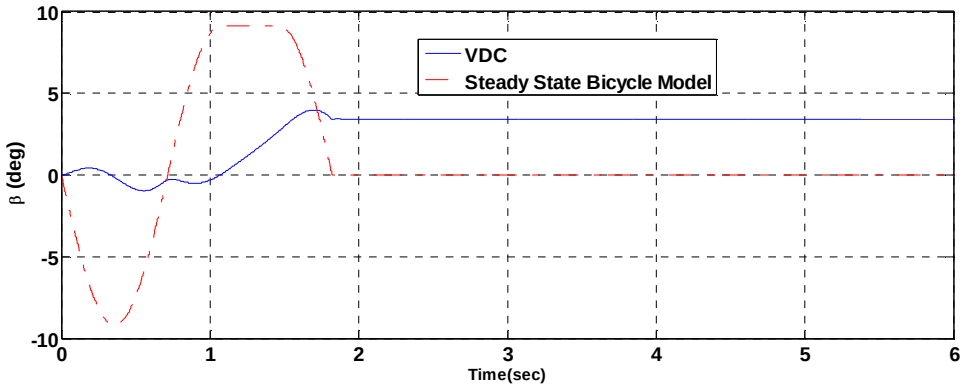


Figure 40 Sideslip Angle Response (Combined (Yaw Rate and Lat. Acc.) Error Feedback with Speed Control on Slippery surface (μ = 0.3))

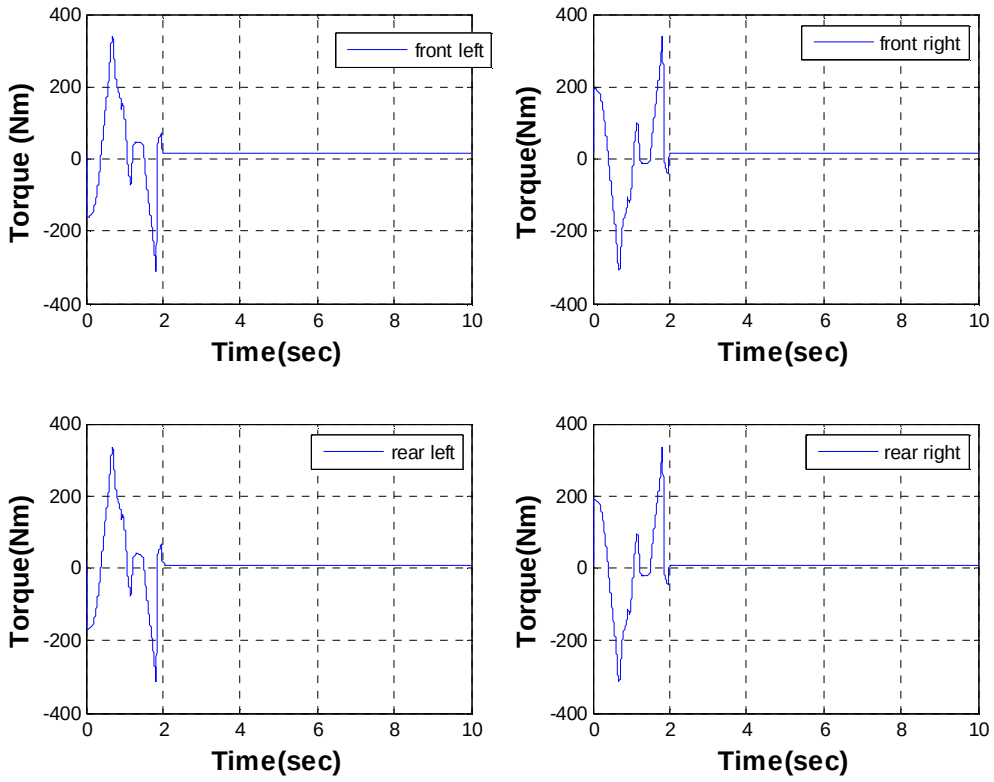


Figure 41 Resultant Torques on Individual Wheels (Combined (Yaw Rate and Lat. Acc.) Error Feedback with Speed Control on Slippery surface ($\mu = 0.3$))

## 4.6 Comparisons (Yaw Rate Control Vs. Lateral Acceleration Control Vs. Combined Control)

To compare yaw moment control through the feedback control variables, yaw rate and lateral acceleration and combined control, simulations were carried out on a slippery surface (low-coefficient of friction, $\mu = 0.3$) without speed control. The initial conditions were set as $v_{x0} = 50$ Kmph and $\omega_0 = \frac{50}{R} = \frac{50}{0.287} = 174.2$ rad/s. Results from the simulations from torque distribution Strategy 4 for each of lat acceleration control and

yaw rate control were plotted against combined control and presented for first few seconds as shown in the figures 41 and 42.

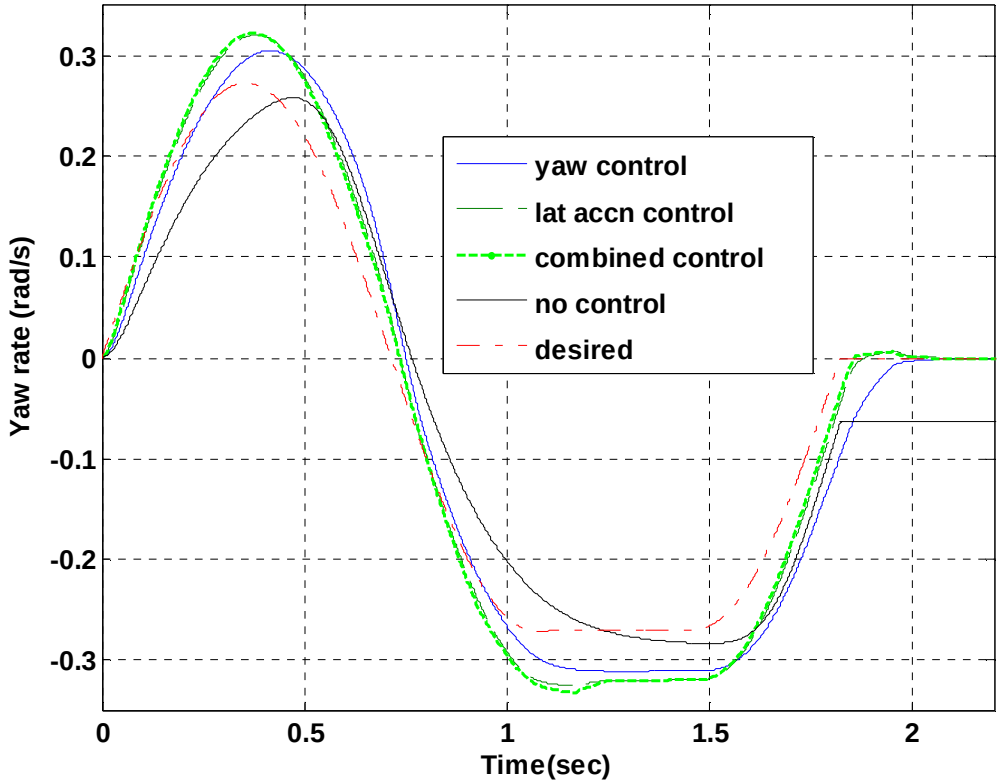


Figure 42 Yaw Rate Response: Comparison of Feedback Control Techniques (Slippery surface (μ = 0.3) without speed control)

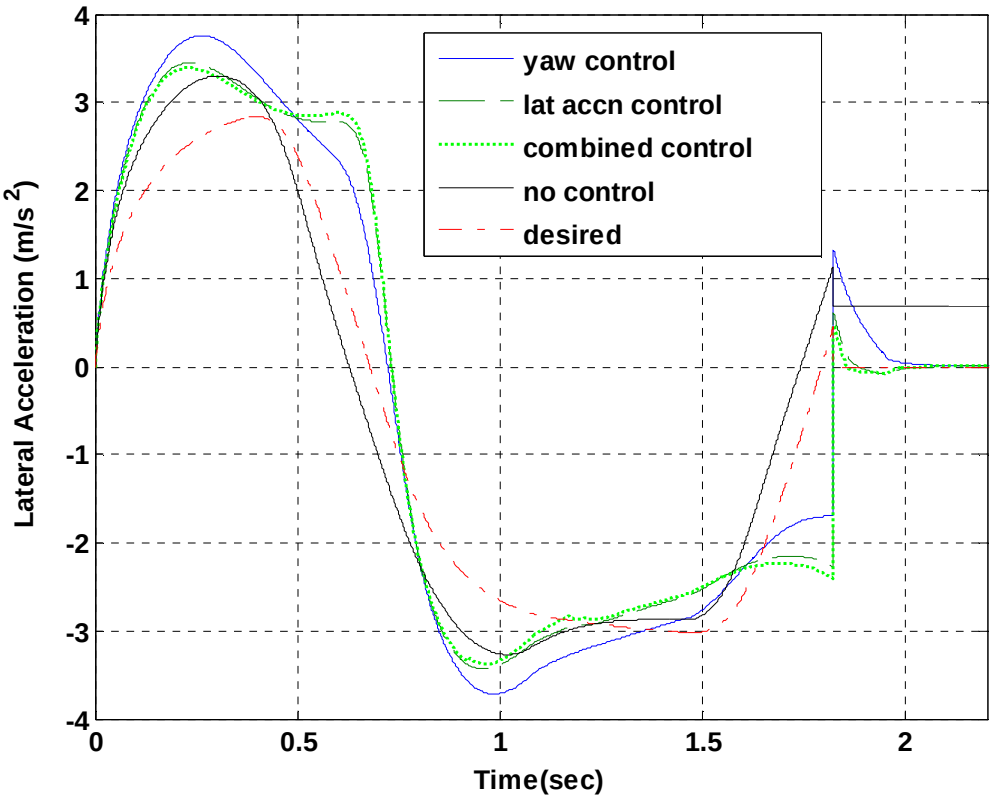


Figure 43 Lateral Acceleration Response: Comparison of Feedback Control Techniques (Slippery surface ($\mu$ = 0.3) without speed control)

The yaw rate and lateral acceleration time history plots for these sets of simulation test conditions don't show any significant differences. The sideslip angle of the uncontrolled vehicle starts deviating at the end of the maneuver and the vehicle can't maintain the desired course while with any of the VDC technique limits the sideways-drift of the vehicle as shown in Figure 44.

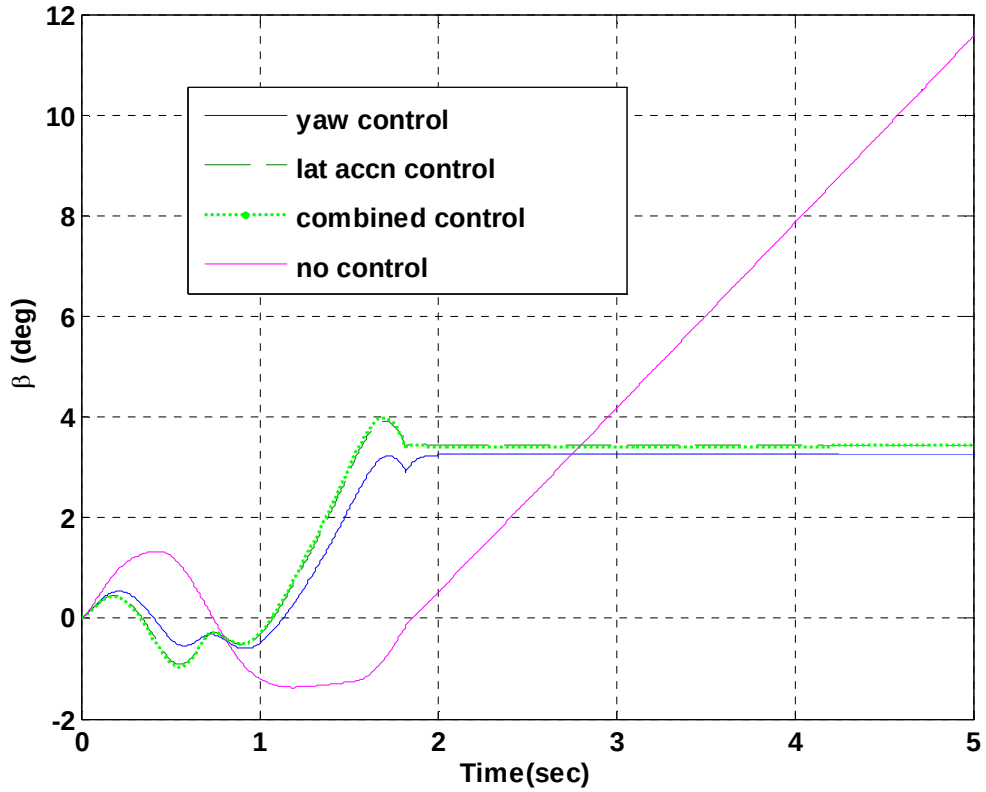


Figure 44 Sideslip Angle Response: Comparison of Feedback Control Techniques(Slippery surface ($\mu$ = 0.3) without speed control)

The comparison of the torque profiles in Figure 45 shows that the combined control produces higher peaks due to high gains chosen for each of the PID gains considered.

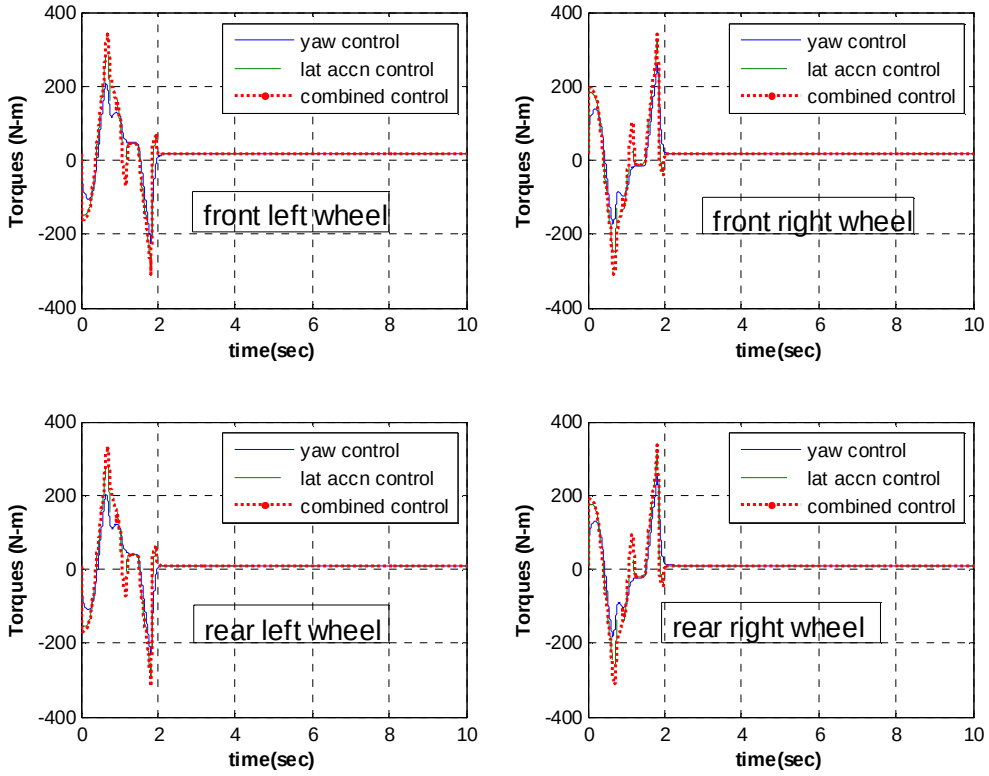


Figure 45 Torques on individual wheels: Comparison of Feedback Control Techniques (Slippery surface ($\mu = 0.3$) without speed control)

## 4.7 Need of Slip Control:

Longitudinal force coefficient $\left(\mu_x = \frac{F_x}{F_z}\right)$ obtained from the Pacejka tire model has been plotted against longitudinal slip ratio S for the corresponding tire (equations 2.25 – 2.28) as shown in Figure 46. The simulation results obtained using different feedback control variables and torque distribution strategies and presented in above sections had the wheel slips falling in the linear region of this curve.

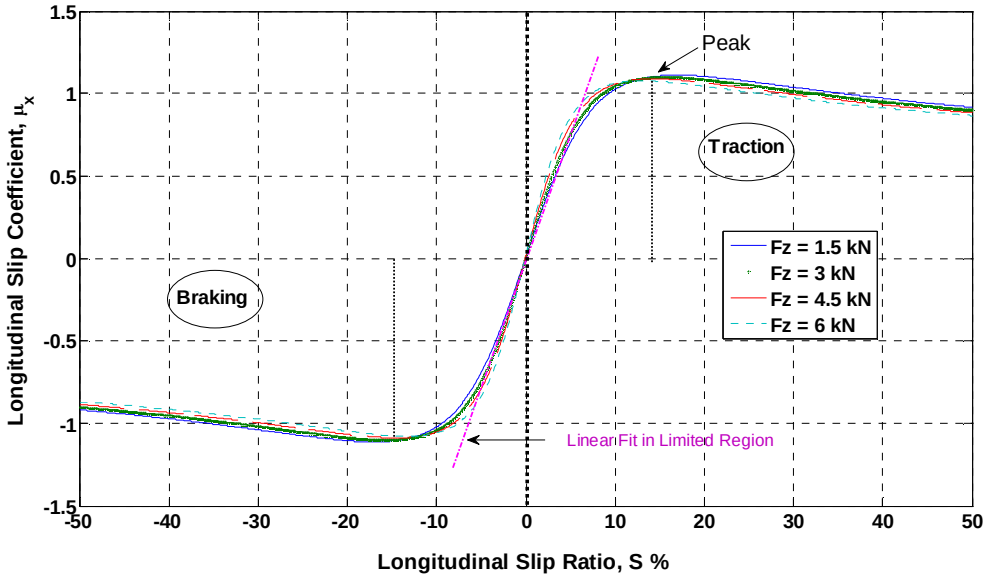


Figure 46 Longitudinal Force Coeff. Vs Longitudinal Slip Ratio: Dry surface (μ = 1)

Although not the focus of this research, an effort was made to control the wheel slip during aggressive cornering maneuvers where the wheels tend to spin or lock up, using PID Controllers and differential torque transfer approach but the results were not encouraging. Some recommendations and suggestions for future research in this area are given in Chapter 5.

## 4.8 Chapter Summary

The chapter presented the simulation results obtained from the different yaw moment control strategies. Standard test maneuvers such as fish hook maneuver, FMVSS 126 ESC test, J-turn were appropriately modified and simulated for evaluating the effectiveness of proposed torque distribution strategies. Effects of road conditions, controller gains and speed controller were studied while analyzing the performance of each torque distribution strategy, comparing different strategies and comparing yaw

moment control through different feedback control techniques. The results showed a good yaw moment control and limiting the sideslip angle for the test conditions considered.

# CHAPTER 5

# CONCLUSIONS AND FUTURE WORK

This chapter provides a summary of the conclusions drawn from the research conducted on independent torque control systems. It also suggests directions for future research to further improve certain performance characteristics of the independent torque distribution management systems proposed in this thesis.

## 5.1 Summary and Conclusions

A restricted but significant amount of study was conducted on independent torque distribution management systems. In conducting this study, a non-linear seven degree-of-freedom vehicle model and a non-linear tire model using Pacejka formulation were adopted. Various vehicle dynamics control architectures were studied and applied to the vehicle model developed using the desired states obtained from the developed bicycle model of the vehicle.

Based on the physical consequence of longitudinal force distribution, two approaches of distribution of torque to each wheel of the vehicle were identified. An approach of differential torque transfer was developed that provided an additional degree of freedom in torque distribution and allowed independent torque control of each wheel. Four torque distribution strategies for achieving the yaw moment control through each of the feedback control variables: yaw rate and lateral acceleration and a strategy combining yaw rate and lateral acceleration control were developed. The simulation responses of the basic vehicle dynamics model include components due to initial conditions of vehicle

states, steering input and applied individual wheel torques. Standard test maneuvers such as fish hook maneuver, FMVSS 126 ESC test, J-turn were appropriately modified and and simulated for evaluating the effectiveness of proposed torque distribution strategies. Effects of road conditions, controller gains and speed controller were studied while analyzing the performance of each torque distribution strategy, comparing different strategies and evaluating yaw moment control through different feedback control variables.

The yaw rate controller was found to be effective in tracking of yaw rate and lateral acceleration of the vehicle on dry and slippery surface conditions. Sideslip angle of the vehicle remained very small and always below the steady state values computed from bicycle model. This rendered separate β-control unnecessary for the test conditions and test vehicle considered. The Strategy 4 (VDC Corrective torques being added to left wheels and subtracted from right wheels) was found to be the best one amongst all distribution strategies considering various control parameters and its ability to achieve the realistic results as presented in Chapter 4 of this thesis. The comparison of feedback control techniques revealed that the three feedback controllers (yaw, lateral acceleration or combined) were very close in terms of achieving VDC for the test conditions considered.

The results in this research constitute first steps towards the selection of a combination of torque-distribution strategy and feedback controller for ensuring vehicle stability with independent drives. The computed torque magnitudes and time responses

can be factored into the design or selection of the electric motors or hydraulic motors for independent drive systems.

## 5.2 Future Work:

Yaw moment control achieved through the different torque distribution strategies and different feedback controllers was found to be effective in tracking desired yaw rate and lateral acceleration on dry and slippery surface conditions for the test maneuvers and test vehicles simulated in this work. The performance of the system can be further enhanced by doing more research focused on the following areas.

More degrees of freedom: The current vehicle model is does not include the suspension. It is recognized that a realistic vehicle model with a realistic suspension model would bring in pitch, bounce and roll of the sprung mass, and the associated dynamic weight transfer effects on the transient handling dynamics. In addition, the effects like roll steer and compliance steer can be studied.

The Pacejka tire model used in this research takes into account the lateral and longitudinal forces and corresponding slips separately. The combined slip conditions should be incorporated to enhance the realistic performance of the system. Together with this, more severe driving scenarios like hard braking in a turn, braking on split-$\mu$ surfaces should be simulated to evaluate the effectiveness of the proposed VDC system. .

Some limited work was attempted on inner-loop on wheel slip control in this work. However, successful simulations were not obtained. More research needs to be carried out to design and successfully implement linear and non-linear controllers for controlling

wheel slips. Finally, the effects of motor (actuator) dynamics should also be included in the simulation model to further understand the hardware requirements of the system.

The upper controllers or torque development systems in this research were simple PID controllers that require fine-tuning of control parameters and gain scheduling to handle different regimes of operation. More robust and non-linear controllers can be designed instead, to control non-linearities and uncertainties in the model more effectively. Reducing control chatter observed in the torque profiles of the torque distribution Strategy 3 (switching of torque addition between the left and right wheels) can make this strategy physically implementable.

Finally, the analysis of the simplified vehicle model in MATLAB/SIMULINK was convenient; the use of vehicle dynamics simulation software like CARSIM can be very useful in including more detail in the vehicle model.

# APPENDIX

## PACEJKA TIRE MODEL: LATERAL FORCE, ALIGNING TORQUE AND LONGITUDINAL FORCE

| Name | Symbol | Units |
|---|---|---|
| Lateral force | $F_y$ | N |
| Self aligning torque | $M_z$ | N.m |
| Slip angle | $\alpha$ | deg |
| Vertical load | $F_z$ | kN |
| Camber angle | $\gamma$ | deg |

1) Lateral Force Equations

$$F_y = D * \sin(C * \tan^{-1}(B * \varphi)) + S_V \quad \text{(A.1)}$$

$$\varphi = (1 - E) * (\alpha + S_H) + \left(\frac{E}{B}\right) * \tan^{-1}(B * (\alpha + S_H)) \quad \text{(A.2)}$$

$$D = (a_1 * F_Z + a_2) * F_Z \quad \text{(A.3)}$$

$$BCD = \left(a_3 \sin\left(2 * \tan^{-1}\left(\frac{Z}{a_4}\right)\right) * (1 - a_5 * |\gamma|)\right) \quad \text{(A.4)}$$

$$B = \left(\frac{BCD}{C*D}\right) \quad \text{(A.5)}$$

$$C = a_0 \quad \text{(A.6)}$$

$$E = (a_6 * F_Z + a_7) * F_Z \quad \text{(A.7)}$$

$$S_H = a_8 * \gamma + a_9 * F_Z + a_{10} \quad \text{(A.8)}$$

$$S_V = (a_{112} * F_Z + a_{111}) * F_Z * \gamma + a_{12} * F_Z + a_{13} \quad \text{(A.9)}$$

2) Longitudinal Force Equations:

$$F_x = D * \sin(C * \tan^{-1}(B * \varphi)) + S_V \quad \text{(A.10)}$$

$$\varphi = (1 - E) * (S + S_H) + \left(\frac{E}{B}\right) * \tan^{-1}(B * (S + S_H)) \quad \text{(A.11)}$$

$$D = (b_1 * F_Z + b_2) * F_Z \quad \text{(A.12)}$$

$$BCD = (b_3 * F_Z + b_4) * F_Z * e^{-(b_5 * F_Z)} \quad \text{(A.13)}$$

$$B = \left(\frac{BCD}{C*D}\right) \quad \text{(A.14)}$$

$$C = b_0 \quad \text{(A.15)}$$

$$E = (b_6 * F_Z + b_7) * F_Z + b_8 \quad \text{(A.16)}$$

$$S_H = b_9 * F_Z + b_{10} \quad \text{(A.17)}$$

$$S_V = 0 \quad \text{(A.18)}$$

3) Aligning Moment Equations:

$$M_Z = D * \sin(C * \tan^{-1}(B * \varphi)) + S_V \quad \text{(A.19)}$$

$$D = (c_1 * F_Z + c_2) * F_Z \quad \text{(A.20)}$$

$$BCD = (c_3 * F_Z + c_4) * F_Z * e^{-(c_5 * F_Z)} * (1 - c_6 * |\gamma|) \quad \text{(A.21)}$$

$$B = \left(\frac{BCD}{C*D}\right) \quad \text{(A.22)}$$

$$E = \left(c_7 * {F_Z}^2 + c_8 * F_Z + c_9\right) * (1 - c_{10} * |\gamma|) \quad \text{(A.23)}$$

$$S_H = c_{11} * \gamma + c_{12} * F_Z + c_{13} \quad \text{(A.24)}$$

$$S_V = (c_{14} * F_Z + c_{15}) * F_Z * \gamma + c_{16} * F_Z + c_{17} \quad \text{(A.25)}$$

The parameters $a_1$ through $c_{17}$ are numerical constants determined by flat track tire tests.

# REFERENCES


1. *Analysis of Vehicle Stability Control(VSC)'s Effectiveness from Accident Data.* **M., Aga and A., Okada.** 2003. proceedings of the 19th international conference on the enhanced safety of vehicles.

2. *The estimated reduction in the odds of loss-of-control type crashes for sport utility vehicles equipped with electronic stability control.* **E.Green, Paul and Woodrooffe, John.** 2006.

3. **IIHS.** INSURANCE INSTITUTE FOR HIGHWAY SAFETY News Release. *http://www.iihs.org/news/2006/iihs_news_061306.pdf.* [Online] June 13, 2006.

4. **Gillespie, Thomas D.** *Fundamentals of Vehicle Dynamics.* Warrandale : SAE Publication, 1992.

5. *Control Aspects of the Bosch-VDC.* **Van Zanten, A.T., et al.** Aachen : AVEC, 1996. International Symposium on Adavanced Vehicle Control.

6. *"Bosch ESP systems: 5 years of Experience".* **Van Zanten, A. T.** Troy : SAE, 2000. SAE Automotive Dynamics & Stability Conference. 2000-01-1633.

7. **Rajamani, Rajesh.** *Vehicle Dynamics and Control.* s.l. : Springer, 2005. pp. 221-256.

8. *Application of active yaw control to vehicle dynamics by utilizing driving/braking force.* **Sawase, Kaoru and Sano, Yoshiaki.** 1999, JSAE Review 20, pp. 289-295.

9. **Kuroda.** *Driving Force Control System in Four Wheel Drive Vehicle. 6* United States, Aug 2000.

10. *All Wheel Drive Independent Torque Control.* **Margolis, Donald L. and Cleveland, Lance.** s.l. : SAE , 1988, SAE. 881135.

11. *Potential of electric wheel motors as new chassis actuators for vehicle maneuvring.* **B.Jacosen.** s.l. : Proceedings of the Institution of Mechanical Engineers Part D, 2002, Journal of Automobile Engineering, Vol. 216, pp. 631-640.

12. *The Hydrid Transmission.* **A.J.Achten, Peter.** s.l. : SAE International, 2007.

13. *Electric Vehicle :Driving Toward Commercialization.* **R.Sims and B.bates.** 1997, Society Of Automotive Engineers.

14. *Dynamic Modeling and analysis of a four motorized wheels electric vehicle.* **E.Esmailzadeh, G.R.Vossoughi and A.Goodarzi.** no.3, 2001, International Journal of Vehicle Mechanics and Mobility, Vol. 35, pp. 163-194.

15. *Integrated chassis control system to enhance vehicle stability.* **A.Ghoneim, Youssef, et al.** 2000, International Journal of Vehicle Design, Vol. 23, pp. 124-144.

16. **Genta, G.** *Motor Vehicle Dynamics, Modeling and Simulation, Series on Advances in Mathematics for Applied Sciences.* Vol. 43.

17. **Wong, J. Y.** *Theory Of Ground Vehicles.* 3rd. s.l. : John Wiley & Sons,Inc., 2001.

18. *Independent Control of All-Wheel-Drive Torque Distribution.* **P.Osborn, Russell and Shim, Taehyun.** 2004. SAE Automotive Dynamics,Stability & Controls Conference. 2004-01-2052.

19. *An experimental examination of j-turn and fishook maneuvers that may induce on-road,untripped light vehicle rollover.* **Forkenbrock G J, et. al.** 2003. SAE. pp. 499-514. 2003-01-1008.

20. *Federal Motor Vehicle Safety Standards;Electronic Stability Control Systems; Controls and Displays.* DEPARTMENT OF TRANSPORTATION, National Highway Traffic Safety Administration (NHTSA), DOT. 2007. Final Rule. Docket No. NHTSA–200727662, RIN: 2127AJ77.

21. **Pacejka, Hans. B.** *Tyre and vehicle dynamics.* second. s.l. : Oxford: Butterworth Heinemann, 2002. pp. 172-197.

22. **Genta, G.** *Motor Vehicle Dynamics, Modeling and Simulation, Series on Advances in Mathematics for Applied Sciences.* 1997. Vol. 43.

# NOMENCLATURE

| | |
|---|---|
| $F_x$ | longitudinal tire force |
| $F_y$ | lateral tire force |
| $F_z$ | lateral tire force |
| $\alpha$ | tire slip angle |
| $\beta$ | vehicle sideslip angle |
| $M_z$ | Total yaw moment acting on the vehicle about the z-axis |
| $v_x$ | longitudinal velocity in vehicle plane |
| $v_y$ | lateral velocity in vehicle plane |
| $a_x$ | longitudinal acceleration in vehicle plane |
| $a_y$ | lateral acceleration in vehicle plane |
| $\delta_f$ | front wheel steering angle |
| T | torque acting on wheel |
| $\omega$ | angular speed of wheel |
| S | longitudinal slip ratio |
| $I_{zz}$ | total vehicle moment of inertia about the z-axis |
| r (or $\dot{\Psi}$) | vehicle yaw rate |
| m | total mass of the vehicle |
| $l_f$ | distance of front axle from C.G. of vehicle |
| $l_r$ | distance of rear axle from C.G. of vehicle |
| l | wheel base |

| | |
|---|---|
| h | height of C.G. of the vehicle above ground |
| $d_f$ | front wheel track |
| $d_r$ | rear wheel track |
| R | wheel radius |
| $M_{Zi}$ | self aligning torque of $i^{th}$ wheel (i = 1,2,3,4) |
| g | acceleration due to gravity |
| $C_1, C_2$ | Cornering stiffmess of front and rear tires (averaged per axle) respectively |
| $K_{us}$ | understeer gradient of the vehicle |
| $K_p, K_i, K_d$ | proportional, integral and derivative gains of the PID controller respectively |
| $\Delta T$ | differential corrective torque to be transferred |
| $e_{a_y}, e_r$ | errors corresponding to lateral acceleration and yaw rate control respectively. |

## SUBSCRIPTS

fl front left wheel

fr front right wheel

rl rear left wheel

rr rear right wheel

L left part of vehicle (includes front and rear left tires)

R right part of vehicle (includes front and rear right tires)

$a_y$ lateral acceleration control

r yaw rate control